QUALITY CONTROL PROGRAMME ON MAMMOGRAPHY SYSTEMS IN THE REPUBLIC OF BENIN: ASSESSMENT OF PATIENTS DOSE OPTIMISATION IN THREE SELECTED FACILITIES

BY

MALICK GERALDO

(ID: 10602725)

This thesis is submitted to the University of Ghana, Legon in partial fulfillment of the requirement for the award of

MASTER OF PHILOSOPHY

IN

MEDICAL PHYSICS DEGREE

JULY, 2018

DECLARATION

This thesis is the outcome of research work carried out by Malick GERALDO in the Department of Medical Physics, School of Nuclear and Allied Sciences, University of Ghana, under the supervision of Dr. Edem K. SOSU, Dr Stephen INKOOM and Dr. Francis HASFORD.

I hereby affirm that, no part of this work has been presented in part or whole to any other University or institution for the award of a diploma, or degree at any level. Accordingly, other works and/or researches done by other researchers cited in this work have been acknowledged under references.

Malick GERALDO Date……
(STUDENT)

Dr Edem K. SOSU Date……
(PRINCIPAL SUPERVISOR)

Dr. Stephen INKOOM Date……
(CO-SUPERVISOR)

Dr. Francis HASFORD Date……
(CO-SUPERVISOR)

ABSTRACT

The Mean Glandular Dose (MGD) was estimated first using Polymethylmethacrylate (PMMA) slabs and secondly MGD was estimated per right craniocaudal (RCC) projection view and left craniocaudal (LCC) projection view. A number of 21 patients out of a total of 28 patients, undergoing breast examination in three (3) selected mammography facilities in the Republic of Benin were involved. Image quality was evaluated based on subjective analysis of images with Leeds Tests Objects and American College Radiology Mammography Accreditation Phantom (ACR MAP). Quality control (QC) tests were performed to verify if the mammography machines selected for the study were working within acceptable level of performance using International Atomic Energy Agency Human Health Series (IAEA HHS) No.2 and No.17 protocols.

The QC tests showed that the mammography units were working within the acceptable performance level.

For the phantom study MGD estimation for all selected mammography systems, the calculated MGD values were below the recommended values, under manual mode as well as the automatic exposure mode. From the comparison of MGD under automatic exposure control (AEC) mode and MGD under manual mode, it was observed that the difference was high. MGD under AEC mode was less than MGD under manual mode and the difference was 1.05 mGy and 1.31 mGy respectively from two (2) mammography units, namely CAR and CHUD/OP.

Data collected from a total of 21 patients was used for MGD calculation. The estimated MGD of patient within the age range of [50 - 64] years with a compressed breast thickness (CBT) of 20 mm for RCC view and 18.7 mm for LCC view reported

a dose of 1.10 mGy, which was slightly high compared to the recommended MGD value for CBT of 21 mm which was 1 mGy. All the remaining estimated MGD was within the recommended international levels of IAEA HHS No.17 protocol. The dose delivered by the selected mammography units were within the acceptable levels of IAEA HHS No.17 for both exposure modes. Thus the AEC mode is recommended because it delivers less MGD and this will help to achieve optimization of patient dose in mammography practices.

DEDICATION

I dedicate this work to my wife ATODJINOU Bethina, to my son Abdel Fadhil Evan GERALDO, to my mother LOCCO Pauline, to my uncle Dr Nassirou GERALDO and to Prof. AMOUSSOU-GUENOU Marcellin.

AKNOWLEDGEMENTS

I am most grateful to my supervisors: Dr Edem K. SOSU and Dr Stephen INKOOM for their effort to make this research feasible. For their direction, guidance and correction made on this work. My thanks also go to Prof. Augustine Kwame KYERE and Dr Francis HASFORD for their infinite encouragement and their help since the beginning of MPhil program. Finally, thanks to all my Medical Physic colleges for their honest collaboration.

TABLE OF CONTENTS

LIST OF TABLES

LIST OF FIGURES

LIST OF ABREVIATIONS

ACR	American College of Radiology
ACR MAP	American College of Radiology Mammography Accreditation Phantom
AEC	Automatic Exposure Control
ALARA	As Low As Reasonably Achievable
CAR	Centre Autonome de Radiologie
CBT	Compressed Breast Thickness
CC	Craniocaudal
CHUD/OP	Centre Hospitalier Universitaire Départemental Ouémé Plateau
COV	Coefficient of Variation
CR	Computed Radiography
DNA	Deoxyribonucleic acid
DR	Digital Radiology
DRLs	Diagnostic Reference Levels
EC	Europeans Commission
ESAK	Entrance Surface Air Kerma
ESE	Entrance Surface Exposure
FFDM	Full Field Digital Mammography
HVL	Half Value Layer
IAEA	International Atomic Energy Agency
IAEA HHS	International Atomic Energy Agency Human Health Series
IAK	Incident Air Kerma
kVp	Tube Voltage peak
kVpset	Tube Voltage set

kVp_{mea}	Measured Tube Voltage
kVp_{dis}	Displayed Tube Voltage
LCC	Left Craniocaudal
LMLO	Left Mediolateral Oblique
mAs	Tube current
mAs_{set}	Set Tube current
mAs_{mea}	Measured Tube current
mAs_{dis}	displayed Tube current
Max	Maximum
MGD	Mean Glandular Dose
MGD_{AEC}	Mean Glandular Dose under AEC mode
Min	Minimum
ML	Mediolateral
MLO	Mediolateral Oblique
MOSFET	Metal Oxide Semiconductor Field Effect Transistor
NBCF	National Breast Cancer Foundation
OD	Optical Density
OBL	Oblique
PMMA	Polymethylmethacrylate
QA	Quality Assurance
QC	Quality Control
RCC	Right Craniocaudal
RMLO	Right Mediolateral Oblique
RPOP	Radiation Protection of Patient
SAA	Saint Anne d'Afrique

SD	Standard Deviation
WHO	World Health Organisation
UK	United Kingdom

CHAPTER ONE

INTRODUTION

This chapter provides a background to normal female breast anatomy, all cancer and particularly to all types of breast cancer. It describes incidence and mortality related to breast cancer worldwide and specifically in Republic of Benin. It also talks about mammography used for early detection of breast disease and the risk of radiation-induced cancer. This chapter also focuses on the statement of the problem concerning breast cancer in Benin and highlights the objectives which would be achieved to fulfil the requirement of this research scope. The relevance and justification of the study are also outlined. The structure followed by the work is also presented at the end of this chapter.

1.1 Background

1.1.1 Female breast anatomy

The breast or mammary glands as shown in Figure 1.1 are modified skin glands which are embedded in the fatty tissue (Tahir, 2001).

The adult female's breasts are paired sub-cutaneous organs on the anterior thorax, lying completely within the superficial pectoral fascia. The breast lies in front of the second to the sixth rib in the mid clavicular line. The breast lies also over the pectoralis major muscle and extends to serratus anterior and external oblique muscle of the abdomen (American Cancer Society, 2017).

The adult female's breasts are made of specific tissue that produces milk (glandular tissue) as well as fatty tissue. The breast portion that produces milk is organized into 15 to 20 sections, called lobes. Each lobe is composed of smaller structures, called

lobules, where milk is produced. The milk passes through a network of minuscule tubes called ducts. The ducts connect and converge into a larger duct that exits the skin in the nipple. The nipple is surrounded by a dark area of skin called the areola (Https://www.webmd.com/women/picture-of-the-breasts#1/2014).

The breast glands are surrounded by a layer of fat tissue and extend through the breast. The adipose tissue provides protection and soft consistency to the breast. The amount of fat determines the size of the breast (Http://www.imaginis.com/breast-health-101-cancer/breast-anatomy-and-physiology 2/1997).

The breast contains also ligaments, connective tissues, nerves, blood vessels, lymph vessels and lymph nodes. Ligaments and connective tissues provides support while nerves are responsible of the sensation (Https://www.webmd.com/women/picture-of-the-breasts#1/2014).

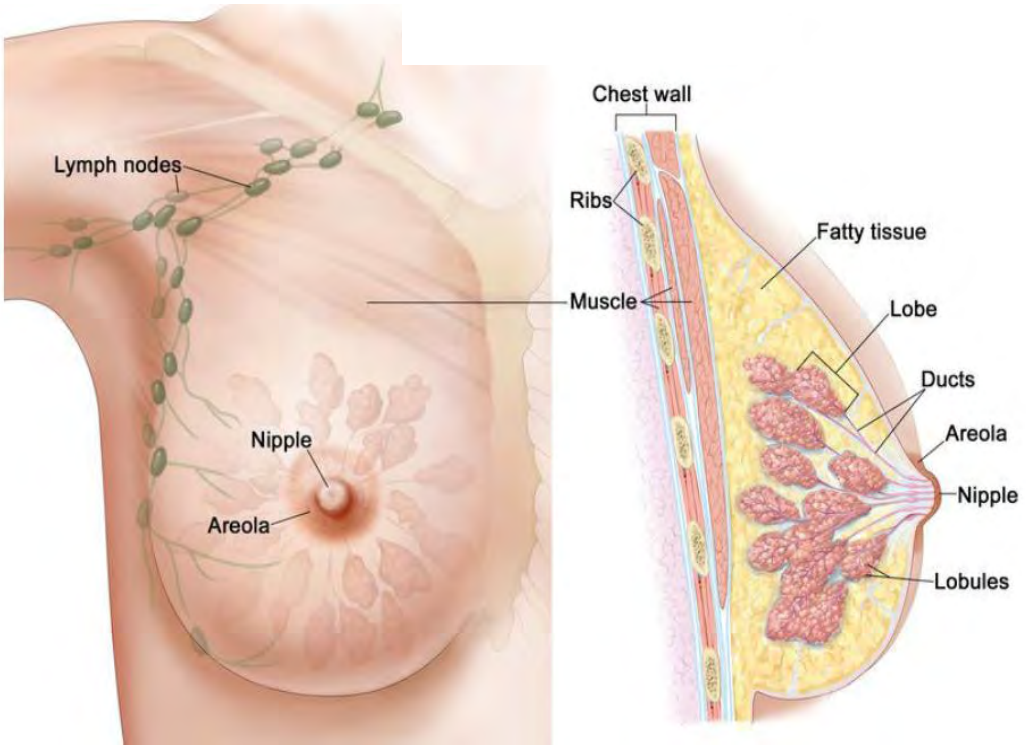

Figure 1.1: Female breast anatomy (www.ncbi.nlm.nih.gov/ 2018)

1.2 Overviews of cancer

Cancer is a disease in which cells in the body grow irregularly, change, or multiply out of control. Usually, cancer is named according to the body part in which it originated. A group of cells resulting from rapidly dividing may form a mass of extra tissue. These masses are called tumors. Tumors can either be cancerous (malignant) or non-cancerous (benign). Malignant tumors penetrate and destroy healthy body tissues. A group of cells within a tumor may also break away and spread to other parts of the body. Cells that spread from one region of the body into another are called metastases (de Rinaldis et all, 2011)

1.2.1 Breast cancer

Breast cancer refers to the proliferation of cells (malignant tumor) that has developed from breast tissue (Breast Anatomy and Physiology | Breast Health 101 | Imaginis - The Women's Health & Wellness Resource Network). There are several types of tumors that may develop within different areas of the breast. Most tumors are the result of benign (non-cancerous) changes within the breast.

Breast cancers can be classified into two main groups: Non-invasive breast cancer and invasive breast cancer (Https://www.webmd.com/women/picture-of-the-breasts#1/2014).

1.2.2 Types of breast cancers

1.2.2.1 Non-invasive breast cancer

Cancer cells that are confined to the ducts and the lobular wall, and do not invade surrounding fatty and connective tissues of the breast. Ductal carcinoma in situ (DCIS) is the most common form of non-invasive breast cancer (90%). Lobular

carcinoma in situ (LCIS) is less common and considered as marker for increased breast cancer risk (de Rinaldis et al, 2011).

Ductal carcinoma in situ (DCIS): is the type of breast cancer in the duct cells that has not invaded deeper or spread through the body as shown in Figure 1.2. Women diagnosed with DCIS have a high likelihood of being cured (de Rinaldis et al., 2011).

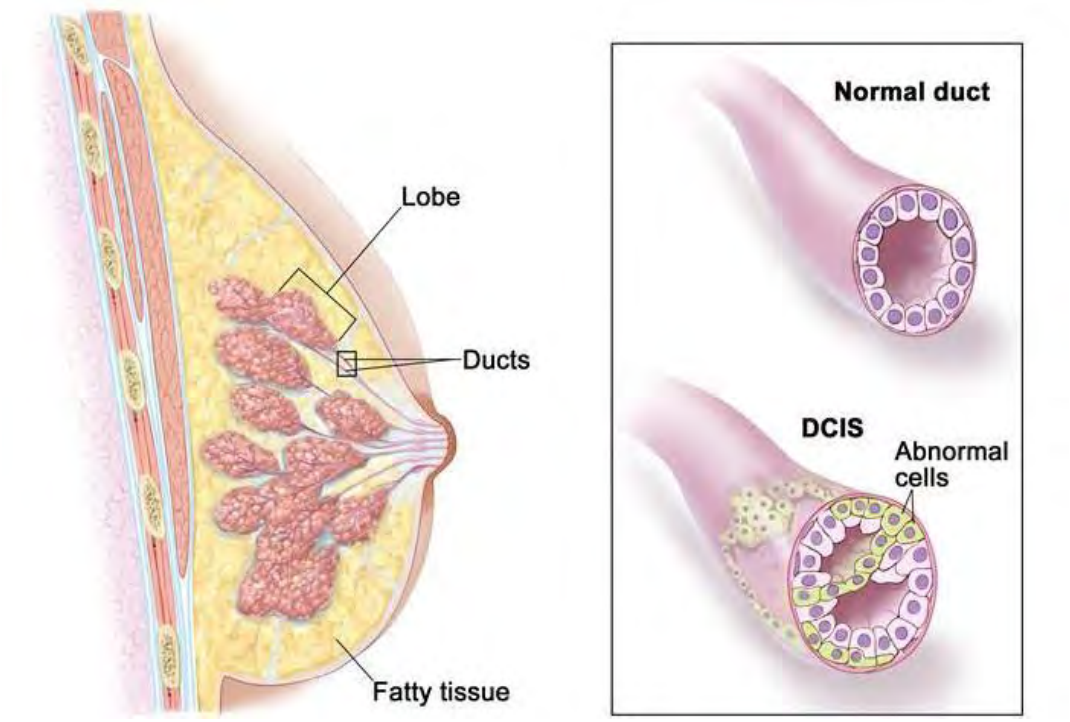

Figure 1.2: Ductal carcinoma in situ (DCIS) (https://www.cancer.gov/news-events/cancer-currents-blog/2015)

Lobular carcinoma in situ (LCIS): although called a carcinoma LCIS, occurs in the milk-producing lobule cells and does not invade or spread and is not a true cancer (Figure 1.3). However, women with LCIS have an increased likelihood to develop invasive breast cancer in the future(de Rinaldis et al., 2011) .

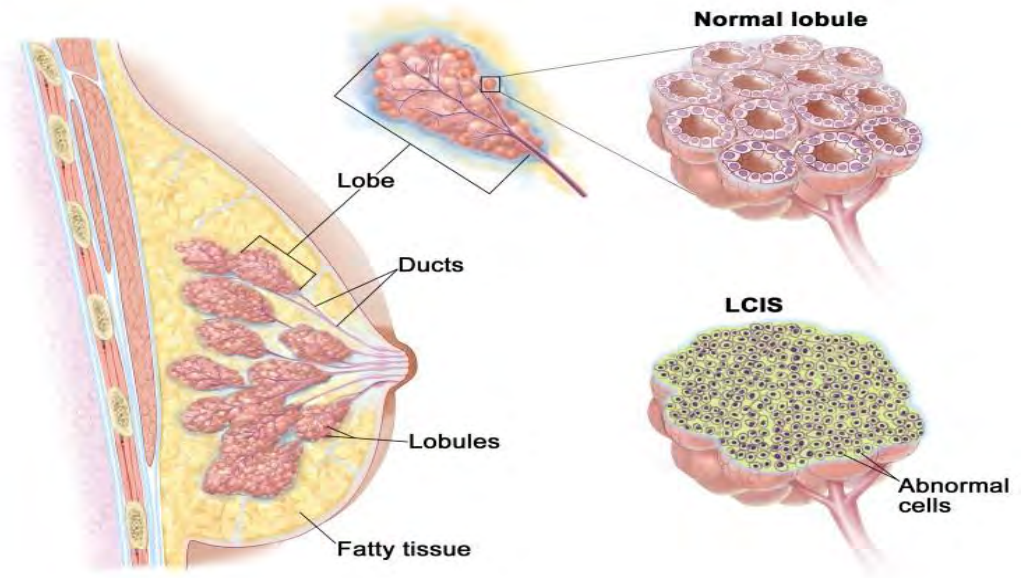

Figure 1.3: Lobular carcinoma in situ (LCIS) (https://www.cancer.gov/news-events/cancer-currents-blog/2015*)*

1.2.1.2 Invasive breast cancer

Cancer cells that break through the duct and lobular wall and invade the surrounding fatty and connective tissues of the breast. Cancer can be invasive without being metastatic (spreading) to the lymph nodes or other organs.(de Rinaldis et al, 2011)

Invasive ductal carcinoma (IDC): is a breast cancer type that begins in the duct cells and invades deeper into the breast, carrying the potential of spreading to the rest of the body (metastasizing) (Figure 1.4). Invasive ductal carcinoma is the most common type of invasive breast cancer.(de Rinaldis et al, 2011)

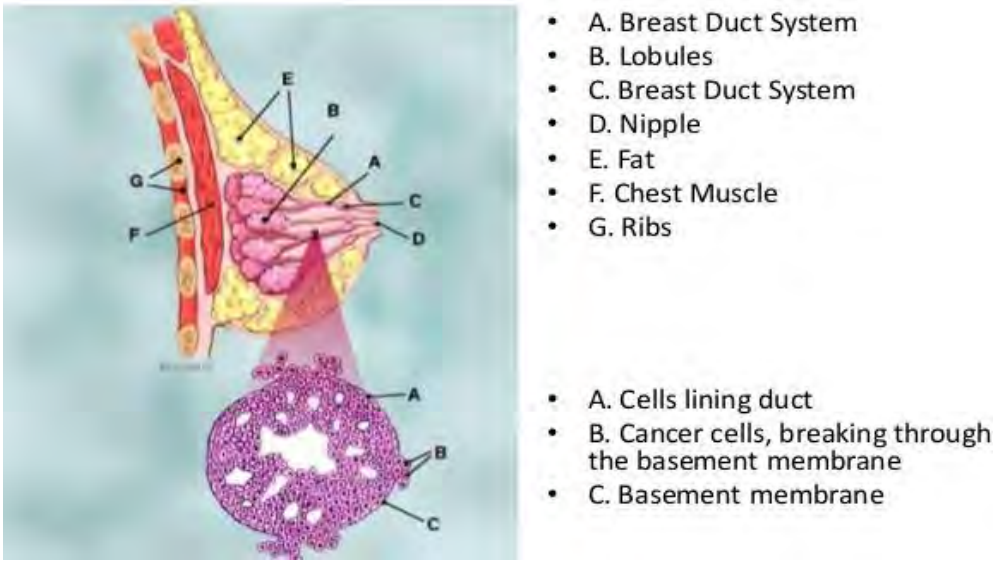

Figure 1.4 : Invasive ductal carcinoma (IDC) (http://healthandsymptoms.com)

Invasive lobular carcinoma (ILC): is a breast cancer type that begins in the milk-producing lobule cells, but then invades deeper into the breast (Figure 1.5), carrying the potential of spreading to the rest of the body (metastasizing). Invasive lobular carcinoma is an uncommon form of breast cancer. (de Rinaldis et al., 2011)

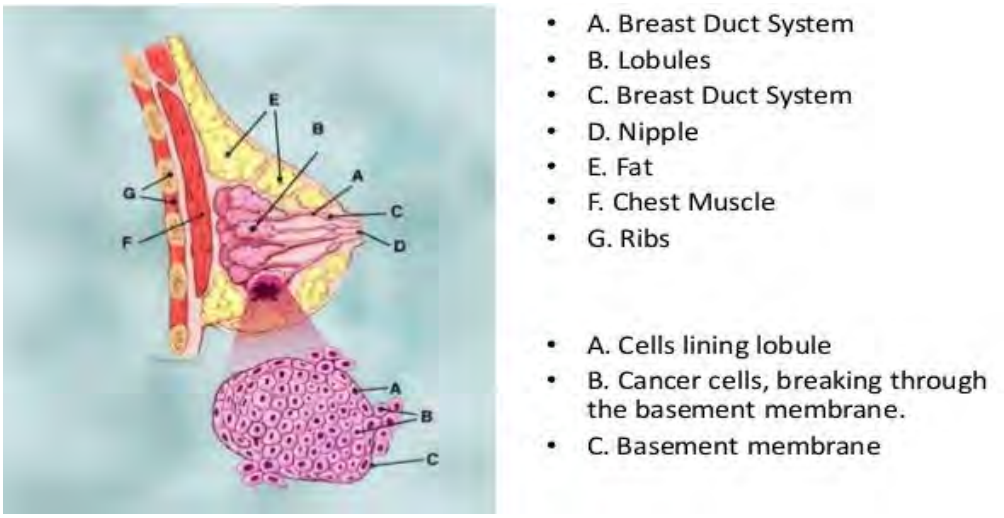

Figure 1.5: Invasive lobular carcinoma (ILC) (http://healthandsymptoms.com)

1.2.3 Breast cancer incidence and mortality

The most commonly diagnosed cancers worldwide were lung (with 1.82 million over all cancers), breast (1.7 million over all cancer) and colorectal cancers (1.4 million over all cancers). It is reported that 14.1 million new cancer cases, 8.2 million cancer-related deaths occurred in 2012 (Ferlay et al., 2015).

Breast cancer is classified as the second most common cancer in the world and, by far, the most frequent cancer among women. An estimated 1.67 million new breast cancer cases (25% of all cancers) were diagnosed in 2012. According to GLOBOCAN 2012 estimations worldwide, 794,000 breast cancer cases are registered in more developed countries while in less developed countries 883,000 breast cancer cases were reported (IARC, 2015).

In Republic of Benin, 910 new cases were registered with 476 death cases in 2012. This high rate of death was registered because 65% of women who have been diagnosed with breast cancer in the Republic of Benin were at the advanced stage of the disease (IARC, 2015).

The best strategy to prevent breast cancer mortality is to find early the breast cancer and get an appropriate treatment. It's easier to treat successfully breast cancer when it found at small size (like a lump that can be felt) and has not spread yet to other organs in the body (de Rinaldis et al., 2011).

1.2.4 Mammography

Mammography refers to X-ray imaging technique designed especially for breast lesions detection (Marianne & Bengt, 2008). Two types of mammography are used. Firstly, the screening mammography performed on women who do not have any breast pathology symptoms, it used to look for abnormal signs that do not appear at

early stage. Secondly, the diagnostic mammography which is performed on women with breast pathology diagnosed from screening mammography or breast changes is seen by a doctor (Committee, 2006).

A mammograph refers to the medical imaging device that used low energy X-ray to obtain detailed image of breast that is recorded on a receptor. When the receptor used is a combination of a film and X-ray cassette, that system is a screen/film mammography system but if the receptor can convert the X-ray to digital image and store it directly on a computer, it is called digital mammography system (Sprawls, 2015).

Mammography requires a highest image quality for all procedures while keeping the radiation dose delivered to the breast, as low as possible. This is only achievable by using optimal equipment and safe procedures. Also, as with any medical examination dealing with ionizing radiation, there is always a small risk of stochastic effect inducing cancer. Therefore, it is vital to be sure that the mammography units used is functioning accurately and the radiation dose delivered to the breast and ascertain whether it falls within international references levels.(Marianne & Bengt, 2008)

1.3 Problem statement

Breast cancer mortality is high in Republic of Benin, 476 out of 910 women lost their life in 2012 (Ferlay et al., 2015). The Republic of Benin has promulgated his nuclear law the March 15th, 2018. Currently there is no a QA/QC program established for the practice of mammography at all in Benin. Whenever mammography equipment goes down,, there are specialized engineers in the maintenance of radiodiagnostic equipment, who are asked to repairs the machines

and then they undertake some performance tests to check how the equipments are operating after repair.

All the existing mammography units have never been subjected to Quality Control tests and mean glandular dose assessment (MGD) has not been done since there was not Medical Physicist available. In most mammography centres, three projection views per breast are performed and the Automatic Exposure Control (AEC) mode is unused. All of these irregularities are not in conformity to International recommendations in mammography practices. These challenges could lead to missed diagnosis and patient overexposure or underexposure.

1.4 Objectives

The main objective of this work was to undertake a comprehensive evaluation of mammography units. The specifics objectives were as follows:

1. Assessment of each mammography equipment assembly function
2. Undertake quality control test of each mammography unit selected for this research
3. Estimate the mean glandular dose to patient breast
4. Evaluation of the image quality of mammograms
5. Comparison of results to European and IAEA standards.
6. Demonstrate the importance of the establishment of a National QA/QC programme of Mammography practice in Benin.

1.5 Relevance and justification

Mammography is considered as the best tool for breast abnormality detection at early stage. Early diagnosis of breast lesions or breast cancer coupled with appropriate

treatment lead to increase survival patients and reduce cancer mortality (Marianne & Bengt, 2008). But to achieve that point, the mammography machine must meet a major requirement which is to produce a high contrast image delivering a minimum radiation dose to breast. A high contrast image is requested because breast lesions and normal tissues have the same density and appear almost identic on the film. The minimum radiation dose is requested for optimization purpose since the breast is one of the most radiosensitive organs and subjected to an uncontrolled exposure can lead to a radiation-induced carcinogenesis (Sprawls, 2015).

For these reasons, it was therefore very important to cross check the performance of existing mammography systems, to estimate the dose delivered to patients undergoing mammography examination under such a conditions of practice in these facilities and to ensure that the mammograms being produced, agree with standards image quality requirements.

1.6 Scope and delimitation

This study involved three facilities located at three different cities in Benin:

1) Sainte Anne d'Afrique (SAA) at Cotonou.
2) Centre Autonome de Radiologie (CAR) at Abomey-Calavi.
3) Centre Hospitalier Universitaire Départemental Ouémé Plateau (CHUD/OP) at Porto-Novo.

A total of 28 patient data was collected from facility CHUD/OP, over the period of three months (from April 2018 to June 2018).

1.7 Organization of the work

This work is composed of five chapters. The chapter one is related to the background; it focussed on the problem statement and defines the objectives of the study. The relevance and the justification as well as the scope of the work were also developed in this chapter. Chapter two reviewed and discussed current literatures published on the topic, works that have been done so far, directly or partially related to this study. Chapter three talked about the different materials, the methods and equations that have been used at various stage of data collection to generate results. The chapter four presented the diverse analysis of collected data and the discussions of the results obtained as well as any new findings. The chapter five as the last chapter, deals with conclusion derived from various outcomes found and their corresponding recommendations.

CHAPTER TWO

2.0 Overview of literature

This chapter provides detailed knowledge of various mammography systems, the importance of quality control on equipment, the benefits of breast examination and the radiation risk related to it. It also discusses about some similar scientific research that have been done.

2.1 Mammography

Mammography is a specialized medical imaging procedure, using low-energy X-ray spectrum to visualize inside human's breasts. Mammography represents the highly effective means to detect breast masses, microcalcifications or to diagnose any other breast diseases in it early stage and to achieve that purpose, a mammography equipment (or mammograph) is designed specifically to produce the best breast image with the highest contrast and spatial resolution and delivering a minimized radiation dose to the breast. It is usually used as well for the screening mammography performed on asymptomatic patient (the patient who does not have any clinical signal of breast disease) as for diagnostic mammography which concerns the medically referred patients. Currently for protection and safety issues two common views per breast are recommended by American and Europeans protocols, craniocaudal (CC) and mediolateral oblique (MLO) views. (Camargo-Mendoza et al, 2011, Dance et al, 2014).

A mammography unit is a best dedicated device for woman breast examination. The generator, the X-ray tube, the compression paddle, the breast support and the receptor with its holder are the different parts of mammography unit. (Figure 2.1).

2.2 The generator

The type of power supply for recent mammography units is specifically of the high frequency or three-phase type and provides an almost constant voltage waveform during exposure. This is needed to lower potential fluctuations and minimize exposure times. Mammography generator power range required is from 3 to 10 kW. (Dance et al, 2014)

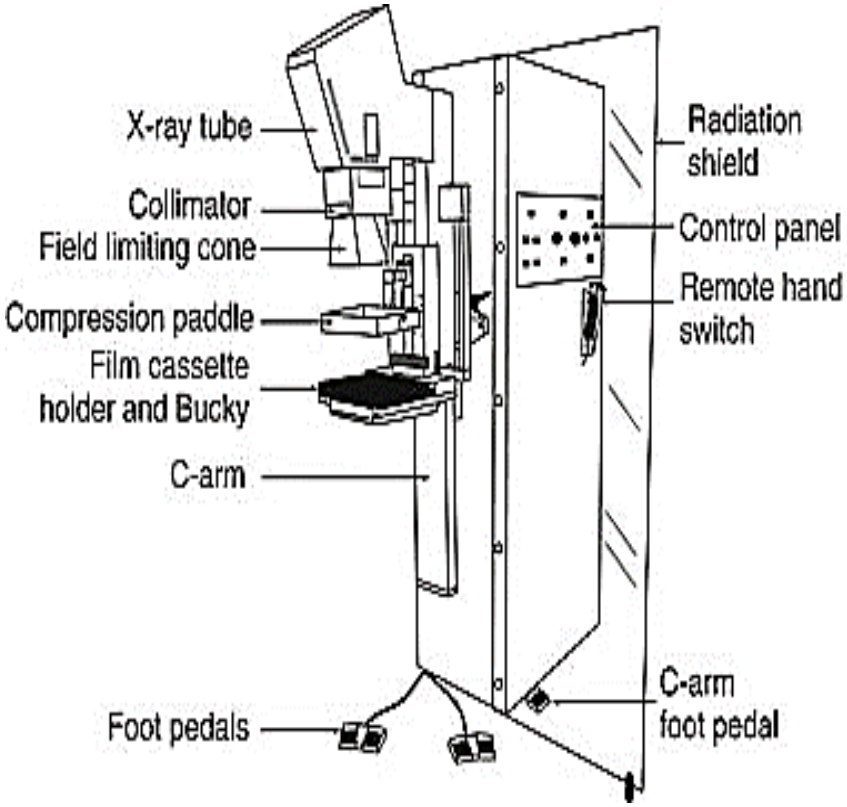

Figure 2.1 : Schematic diagram of a mammography unit (https://clinicalgate.com)

2.2.1 The tube

Most of the mammography X-ray tubes use an anode/filter combination to improve the quality of the mammogram and keep lows as possible the dose of radiation delivered to patients(Sprawls, 2015).

2.2.2 Spectrum

For breast imaging, the ideal X-ray spectrum needed must be composed of mono-energetical photons (all photons have same or almost same energy) and can be adjusted for different breast conditions (thickness and density). For each breast condition it should be an optimum photon energy that will produce the high image contrast by delivering optimized dose to the breast.

In the case that the spectrum (photon energy) decreases below the optimum energy, the dose delivered to the breast will increase due to the weakness of the radiation penetration through the breast.

If the spectrum (photon energy) increases above the optimum energy the contrast will decrease because of the increased penetration through the glandular and pathologic tissues. The most common spectrums used in mammography (Sprawls, 2015) are molybdenum/molybdenum spectrum (Mo/Mo) (Figure 2.2), molybdenum/rhodium spectrum (Mo/Rh) (Figure 2.3) and rhodium/rhodium (Rh/Rh) (Figure 2.4).

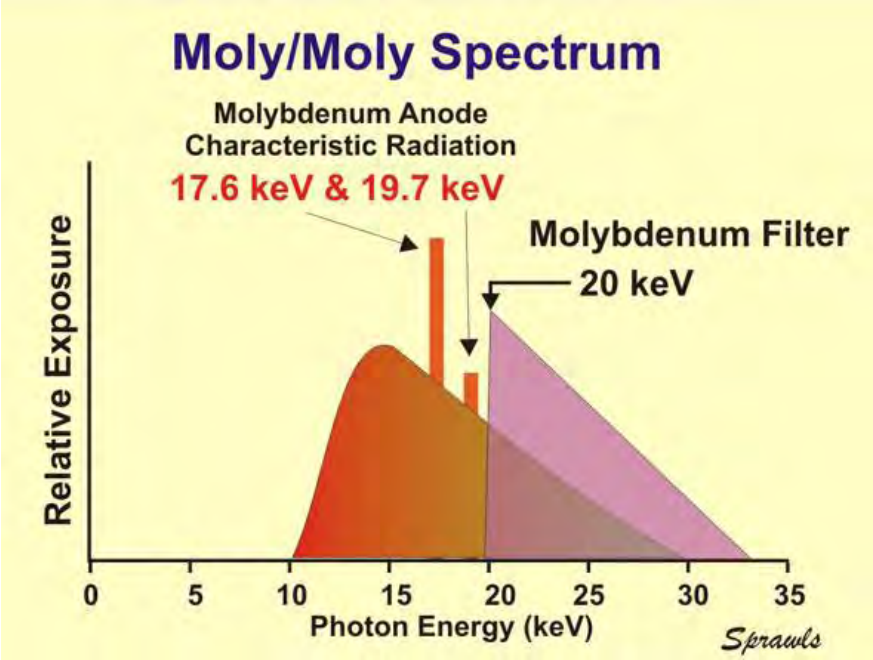

Figure 2.2: Mo/Mo Spectrum (Sprawls, 2015).

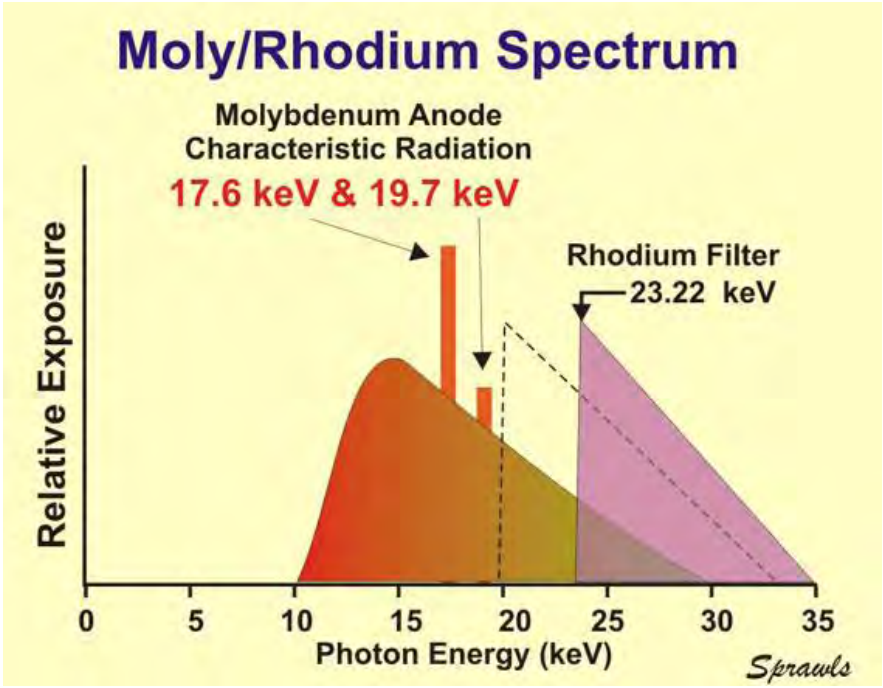

Figure 2.3: Mo/Rh Spectrum (Sprawls, 2015).

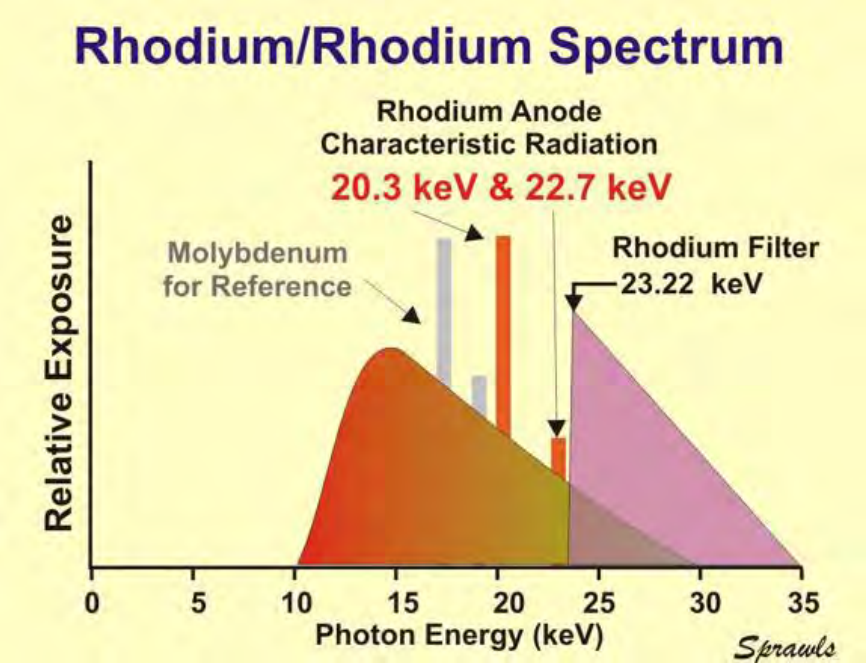

Figure 2.4: Rh/Rh Spectrum (Sprawls, 2015).

2.2.3 Anode material

The tube uses the rotating or fixed anode type in which electrons coming from cathode, impinge the anode target material at a specific point called focal spot which is situated on the target surface.

For better visualization of common mammary tissue, the radiation energy level that produces a higher images contrast must be approximately 20 keV (Sprawls, 2015).

Molybdenum (Mo) and rhodium (Rh) targets are commonly used as target materials because they generate appropriate characteristic X-ray radiation that is useful for mammography purpose. Molybdenum generates characteristics X-rays energy of 17.9 and 19.5 keV and rhodium produces characteristic X-rays energy of 20.2 keV and 22.7 keV. The X-ray radiations generated by rhodium provide appropriate penetration of thicker or dense breast. The tube peak voltage, that allows these characteristic X-rays to be produced, must be higher than these values. It usually ranks from 25 to 35 kVp (Sprawls, 2015).

2.2.4 Filtration

Mammography filtration is based on the "k-edge" principle which allows to get close to the optimum X-ray spectrum needed for mammography. The K-edge energy means the binding energy of k-shell electrons of filter material. The usual filter material used in mammography is molybdenum (Mo), but some devices also have alternative rhodium (Rh) filter that can be selected. The objective of using filtration is to remove most of the X-ray that have energy above the k-edge energy for specific filter material, either molybdenum or rhodium, this would aid to get the suitable penetration and a high image contrast. Filtration is also used to take out the very low energies of radiation which do not contribute to image quality but will only increase the patient dose (Sprawls, 2015).

It is recommended that the molybdenum filter must be only combined with the molybdenum anode and the rhodium filter can be combined with both the molybdenum and rhodium anodes (Sprawls, 2015).

2.2.5 Compression

One of the essentials of effective mammography is a good breast compression (but without pain) during the mammography examination using the compression paddles which is made of a radio-transparent paddles having an X-ray transmission of approximately 80% at 30 kVp. Compression in mammography has various advantages.

It gives more breast thickness uniformity leading to the best fit of exposure into the film latitude and dynamic range. It also spreads breast tissue out, making easier pathology to be detected and brings the breast closer to the image plane, minimizing image magnification and focal spot blur. It reduces patient motion avoiding kinetic

blur. It reduces the breast thickness and allows low peak voltages to be used, therefore improving image contrast and sharpness. The compression reduces also scatter radiation and improves image contrast minimizing radiation dose delivered to the breast (Sprawls, 2015, Dance et al, 2014).

2.2.6 Grid

Scatter radiations increases with breast thickness and peak voltage. As any other X-ray procedure, mammography uses the anti-scatter grid (Figure 2.5) to remove scattered radiation for the purpose of get high image quality. Mammography is normally performed using a moving grid or Bucky. Compared to grids used in general radiology, mammography grids have lower grid ratios and the interspacer materials between the strips are selected to absorb very low X-ray energies. Grid ratio is calculated dividing the height (h) of the lead strips by the width (w) of interspacer materials. The typical grid ratios are 4/1 or 5/1 for moving grid (Sprawls, 2015, Committee, 2004).

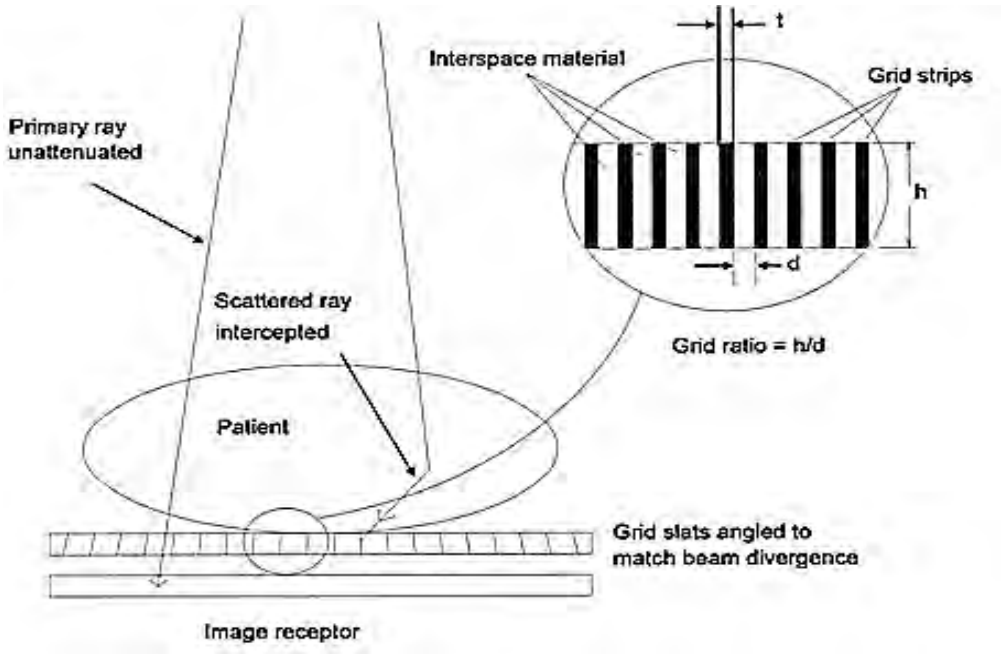

Figure 2.5: Mammography antiscatter grid scheme and function (Sprawls, 2015).

2.2.7 Receptor

There are two distinct mammography methods based on the manner the mammograms are recoded and displayed: conventional (screen-film) mammography and digital mammography. Each has different design features which help to achieve image quality.

For screen-film mammography, low-dose X-ray is used to produce detailed images of the compressed breasts between a compression plate and the breast support. The film is placed inside an X-ray cassette. It is used as image recorder, transporter and store. It is the image display device. The important point is that the film contrast cannot be modified or adjust after exposure. It is processed chemically. The film (mammogram) is viewed by the radiologist on a viewing box (Sprawls, 2015).

Digital mammography also uses X-rays to produce breast images, but unlike the conventional system, its detector converts X-ray image to digital images and then images are directly memorized in a computer. That image can be improved, magnified and exploited for further evaluation. The digital mammography has more advantage than the film-screen mammography (Sprawls, 2015).

2.3 Automatic exposure control (AEC)

Automatic exposure control (AEC) also known as photo timing, is an inherent function of the mammography machine, conceived to produce automatically the appropriate radiation exposure that may produce an acceptable and consistent image contrast. It is one of the mammography function mode which can control the tube loading automatically and terminate the exposure as soon as the pre-set sensor (dose

detector) located under the image receptor is reached (Ślusarczyk-Kacprzyk et al., 2016, IAEA, 2014, Dance et al., 2000).

Most of later-day mammography systems have the AEC mode. The AEC sensor is located normally behind the image receptor to avoid the attenuation of the incident X-ray beam and the formation of its own X-rays shadow which is especially significant due to the low energy beam used in mammography. Placed behind the image receptor, the AEC sensor measures the exposure of radiation that attends the image receptor passing through the breast. The AEC sensor is also able to terminate the exposure when sufficient radiation exposure has been delivered to produce desired film density. For each technique, as the breast thickness varies (from 2.5 cm to 11 cm) and as the peak kilovoltage varies (from 25kVp to 35 kVp), the AEC system should be able to maintain the optimum optical density within a standardized range of optical density. Also, there are adjustments to provide proper compensation for different film-screen combinations. For many mammography units, the position of the radiation detector can be varied between two or more predetermined positions to facilitate the exposure of breast of different size and density (Jaffe, 2015, Assiamah et al., 2005).

2.4 Magnification

A magnification means aggrandizement of a suspicious area found on a mammogram. A magnification mammography is performed to examine and count the number of micro-calcifications. It is also useful to check the tissue structures of the suspicious area and their borders, using a magnification device which, bringing the breast closer to the radiation source increases the distance between the breast and

breast support. This helps to acquire an enlarged image of the region of interest: it is called a magnified mammogram (Hacking et al., 2000).

2.5 Recommended breast examinations

American College of Radiology (ACR) recommended in mammography practice two common breast X-ray examinations: screening mammography and diagnostic mammography.

2.5.1 Screening mammography

The screening mammography is a periodic X-ray examination. It is performed annually (for 40 to 74 years) or biennially (for 50 to 74 years), on women who do not present any symptoms of breast lesions. The main purpose of screening mammography is the detection of unsuspected breast cancer at a early stage. The direct consequence of this early detection is the reduction of breast cancer death rate because breast cancer is highly curable when detected early (Miglioretti et al., 2016). There also exist a special screening mammography concerning a woman who refers herself for medical services and who does not have an identified referring physician or other healthcare provider. It called Self-referral mammography (Committee, 2004a).

If there is any abnormality on the mammogram, additional investigations will be requested, but these do not perforce mean that it is breast cancer. About 5% of women who undergo a screening mammography need additional breast examination to clarify an abnormal finding on the previous mammograms. These additional investigations are usually further breast examinations such as mammography and/or breast ultrasound. Some women may also need a needle biopsy for more clarification of the finding. The needle biopsy means a small piece of breast tissue is removed and

checked for any abnormality using a fine needle introduced into the breast. In some rare cases, a surgical biopsy is required to confirm whether cancer is present (Monticciolo et al., 2017).

2.5.2 Diagnostic mammography

A diagnostic mammography is breasts X-ray examination performed on women who have a symptom such as skin changes, nipple discharge, lump or tenderness that is discovered within the breast by their doctor or another health professional. This mammogram objective is to confirm whether the unusual signs observed clinically are benign and therefore there is no need of treatment or whether the changes are cancerous (breast cancer) and further tests and treatment will be required.

Breast examination is performed using a mammography machine also called a mammograph. It is a dedicated X-ray tube machine especially designed for breast abnormality investigation (Shah et al, 2012).

An ionizing radiation such as X-rays, have ability to cause harm effects (Stochastic effects) within human organisms. The glandular tissue represents the more radiosensitive and active part of the breast. Its tissue-weighting factor is 0.12, which means woman breast is one of the organs having the most radiosensitivity in the body. (Sosu et al., 2018, Monticciolo et al., 2017, Aggarwal, 2016).

2.6 Interactions of X-ray with matter

X-rays photons are considered as individual units of energy. When X-rays beam traverse a medium, some of the photons interact with the particles contained within the medium and their energy can be either absorbed or scattered. In another case the

photons can go across the medium without interaction with any particles (Nikjoo et al, 2012).

X-rays radiation is classified as an indirect ionizing radiation because interacting with an object it produces charged particles that in turn will ionize the matter. There are three major kinds of X-rays interactions with matter photoelectric effect, Compton scattering and pair production.

2.6.1 Photoelectric effect

The incident X-ray photon has energy that is slightly higher than the binding energy of the inner-shell electron of an atom. This interaction occurs only when the photon has enough energy to dominate the binding energy. In this process, the photon cedes its total energy to an inner-shell electron contained in the matter's atom and disappears. This incident photon's energy lost is divided into two parts. A part of the energy serves to break the inner-shell electron binding and to snatch it from its orbit. The remaining energy is transferred, as a kinetic energy to the electron which is ejected out of the atom (Nikjoo et al., 2012).

2.6.2 Compton scattering

The photon can also interact with an outer-shell electron contained in the matter's atom. It releases a part of its energy to outer-shell electron which is ejected out of its orbit and then it is deflected (scattered) from its initial direction (Nikjoo et al., 2012).

2.6.3 Pair production

This interaction occurs only if the incident photon energy exceeds 1.022 MeV. The photon interacts with the nucleus in such a way that its energy is converted into

mater. The outcome if the interaction is the production of a pair of particles an electron or negatron and a positron. These particles have the same mass and each equivalent to rest mass energy of 0.511 MeV. This kind of interaction is not commonly encounter in radiodiagnostic procedures (Nikjoo et al., 2012).

Other possible interaction mechanisms are coherent scattering where there is any photon energy transferred or deposited. Therefore, photoelectric effect, Compton scattering, and pair production are the most important interactions in radiations dosimetry as they lead to partial or complete transfer of photon energy to electron energy which in turn transfer energy into matter. (Sprawls, 2014). The amount of photon energy deposited or transferred through the medium depends on the thickness, density and atomic number of the absorbing medium and on the energy of the incident photon. (Davisson, 1968).

The interactions of X-ray have a great importance in diagnostic imaging for many reasons. For example, radiographic images come from interactions of X-ray photons with different anatomic structures of human's body, and the interaction of photons with the receptor converts an X-ray image into one that can be viewed or recorded.

2.7 Biological effects of X-rays Radiation

A radiation is defined as the process of emission or transmission of energy. Radiations can be classified into two principal groups: non-ionizing radiation and ionizing radiation. Ionising radiation which is most concerned in this study consists of particles from atom or electromagnetic waves that are energetic enough to eject electrons from atoms or molecules. Then the outcome of electron is production of ion. Examples are alpha particles, beta particles, neutrons, gamma rays, and X-rays (Sprawls, 2014).

Ionization of an atom is the removal of one of its orbital electrons. When an electron is removed, two charged particles, the free electron, which is electrically negative, and the rest of the atom, which bears a positive charge, are produced. These are called an ion pair. Ionizing radiation has sufficient energy to cause chemical changes in cells and damage them. Some cells may die or become abnormal, either temporarily or permanently. Radiation can cause by damaging the genetic material (DNA) contained in the body's cells. The extent of damage to the cells depends on the amount of and duration of the exposure, as well as the exposed. Very large amount of radiation exposure can cause sickness or even death within hours or days. In general, the amount and duration of radiation exposure affects the severity or type of health effect. Current studies suggest there is some cancer risk from any radiation. (Hendrick, 2010).

2.7.1 Radiation-induced cancer

As all examination using ionizing radiation, there always exists a tiny stochastic risk to radiation-induced carcinogenesis. Radiation-induced cancer results from different cells in which the control system has been damaged by ionizing radiation trough chromosomal aberrations or gene mutation. Those damages may provoke cells multiplication and growth in an uncontrolled way (over proliferation) resulting in radiation – induced cancer.

Since a century, it is known that ionizing radiation causes cancer in human body. The first radiation-induced cancer incidence was reported in 1902 (Shah et al., 2012).

Radiation-induced breast cancer is a stochastic (late) effect caused by cumulative exposure to low energy radiation over a long period of time during screening mammography examination (Aggarwal, 2016).

2.8 Quality Control in mammography procedure

2.8.1 Quality assurance (QA)

It refers to all those planned and systematic actions necessary to provide adequate confidence that a structure, system or component will perform satisfactorily in service. This refers to the optimum quality of the entire diagnostic process; consistent production of adequate diagnostic information with minimum exposure of both patient and personnel (IAEA, 2009).

2.8.2 Quality Control (QC)

It refers to the technical aspects of mammography and it is evaluated by following described protocols and performed by either the radiologist or Medical Physicist (Hogge et al, 1999). It includes monitoring, evaluation, and maintenance at optimum levels of all characteristics of performance that can be defined, measured, and controlled. The evaluation of equipment must address the various critical stages of the imaging chain, that is, acquisition, processing, and display. Because of the relevance of mammography in accurately diagnosing breast cancer, especially in its early stages, and reducing high mortality rate in women, it is essential that all mammograms be performed and interpreted with the highest possible quality standards. QA and QC measurements and guidelines must be present in all mammography facilities. These guidelines must be strictly adhered to, in order to assure accurate diagnosis for all patients. The importance of QC on the equipment is

to assure that images are not degraded with artefacts that may mimic microcalcifications. It is also to assure that view boxes and viewing conditions are optimised and maintained at an optimal level. It is also to assure that the breast dose is As Low As Reasonably Achievable (ALARA) for the mammographic information required (Pwamang, 2016, Reis et al., 2013).

2.9 Mammography Dosimetry

There is a significant risk of radiation induced carcinogenesis associated with mammography. The determination of mean glandular breast dose forms an important part of the quality control of mammography imaging systems since it gives an indication of the performance of the imaging system as well as estimating risk to the patient. Because of the fact that breast cancer almost always arises from the glandular tissue of the breast, and also based on the assumption that it is the glandular tissue in the breast that is most sensitive to radiation effects. The average radiation absorbed dose of the glandular tissue is used to measure the radiation risk associated with mammography (IAEA RPOP- 2013). The MGD is defined as the average dose to the glandular tissue. It is not easy to estimate the MGD directly, so the entrance surface air kerma (without back scatter) at the upper surface of the breast skin is determined and the MGD is calculated by multiplying by appropriate conversion factors following equation (2.1)

$$MGD = K.g.c.s \qquad (2.1)$$

Where K is the incident air kerma (without back scatter) at the upper surface of the breast, g is the incident air kerma to mean glandular dose conversion factor (g-

factor), c corrects for any difference in breast composition from 50% glandularity and the factor s corrects for any difference due to the use of a different X-ray spectrum. The conversion factors g, c and s can be interpolated or extrapolated from the work of Dance et al 2000, 2009, and 2011.

2.10 Overview of Related Works Done

Patient doses and image quality are the major concerns in mammography. Breast cancer screening, where most of the patients do not have any health issue and where any small change or lesions of the mammary tissues are looked for. High image contrast and resolution are requested because normal breast structures and pathologies appear almost identical. Although mammography uses low kilovoltage X-rays for breast imaging, dose estimation is very important because the risk of radiation-induced carcinogenesis exists. Therefore, the assessment of the equipment performances such as the QC tests must be done to assure the optimized radiation protection in the mammography practices.

A lot of work has been done across the world, on mammography dose assessment, and/or image quality including both of conventional systems and digital systems.

Sosu et al in 2018 conducted a research entitled: Determination of dose delivery accuracy and image quality in full-field digital mammography (FFDM), in Ghana. The objective of this work was to evaluate the global performance of the first full-field digital (Fujifilm-Amuletf) mammography unit in Ghana by performing through a comprehensive quality control assessment in the order to optimize mammography procedures and patient radiation protection. The quality control tests including unit assembly, output repeatability and linearity, kVp accuracy and repeatability, Half-

value layer, exposure parameters, AEC, image quality tests and MGD estimation were carried out following the International Atomic Energy Agency (IAEA) Human Health Series No.2 and No.17 protocol and the European guidelines for quality assurance in breast cancer screening and diagnosis. Also, the ImageJ software with the "Rose Model" was used to analyse the images. The results from the QC tests performed indicated that the mammography unit was functioning correctly. The image quality test based on the Signal-to-Noise and Contrast-to-Noise values, determined from images showed that the images agree with standard quality. All the MGD estimated or displayed on the system fell below the standard level except the displayed MGD (7.17 mGy) for the 90 mm breast thickness, which exceeded the standard limit. The mammography X-ray equipment at the Korle-Bu teaching Hospital, Accra Ghana was then recognized to work under optimized conditions and was therefore recommended for further usage.

In Ghana, Akrobortu et al. (2013) did an inter-comparison of dose indicators and mean glandular dose for some selected diagnostic mammography units in Accra, Ghana. The studies were carried out in three facilities in Accra and on all 300 patients (100 from each facility) were selected at random for the MGD estimation. Mammography screening and diagnostic examinations were performed by specialists (radiologists) and qualified radiographers at the respective facilities. Quality control measurements were carried out on the three mammography units using standard performance criteria. Darkroom quality control and some of quality control tests with respect to: tube voltage accuracy and reproducibility, radiation output linearity and consistency, MGD to patients were assessed for each unit. MGD estimated from free in air measurements were found to be 0.32 - 1.45 mGy, 0.33 -1.30 mGy and 1.05-

2.70 mGy with grid for facilities A, B, and C respectively using a standard breast thickness of 45 mm. The performance criteria of key quality control parameters were found to be within acceptable limits except base + fog and contrast index of radiographic films.

In Kenya, Wambani et al. in 2011 assessed patient doses during mammography practice at the Kenyatta National Hospital. The study was carried out over a period of one year where the annual numbers of mammography examination were counted from the hospital patient records. The objective of the study was to evaluate the MGD in mammography for craniocaudal (CC), mediolateral oblique (MLO) projections and the dose per woman. A mammography equipment performance test was done based on quality control parameters. Viewing box luminance and room luminance were assessed as well as image quality on each mammogram. All the quality control tests performed were passed except luminance and ambient light. The viewing boxes were less bright while ambient light in the reporting room was too bright to the extent that it may affect the level of viewing diagnostic information in the mammograms. In the end, there were 3264 films from 1252 women of between 25 to 90 years old. The MGD per film was 2.14 mGy (range 0.27-9.43 mGy) for the CC projection and 2.44 mGy (range 0.20-10.12mGy) for the MLO projection 17% of CC films and 30% of MLO films recorded doses above the 3mGy diagnostic reference level. There were high image quality scores in this study due to the skilled technologist and regular quality control tests performance.

In Ethiopia, Seife et al. in 2012 did an evaluation of mean glandular dose during diagnostic mammography examination for detection of breast pathology, in Ethiopia.

The study was done in a period of ten months. Five mammographic units were included in this study. From 51 breast patients of all CBT values, clinical data were collected. Exposure factors for each mammogram was collected and the MGD was estimated making use of the ESAK and tabulated conversion factors. The maximum to minimum ratio of the average MGD recorded in the units was 4.71. The MGD to breast dose was found to vary from 0.23 mGy to 7.89 mGy, with 16.5% of the dose above the upper limit of the ACR recommendation established for the medium-sized breast of 4.2 cm CB. The need for strict quality control was recommended.

In 2006 in the lower region of Northern Thailand, Sookpeng and Ketted have conducted a study on MGD from routine mammography. MGD was estimated per craniocaudal (CC) and mediolateral oblique (MLO) views for each breast and the total dose determined for both breasts per woman among 2060 views from a population of 515 women undergoing mammography examination. Six selected mammography units were used in this study. Quality Control tests such as kVp, exposure time and half value layer's (HVL) accuracy and repeatability were performed on the machines and all of them have got acceptable tolerance compared to ACR standards. Patient data were collected and recorded taking account of Compressed Breast Thickness (CBT) for each projection. The kVp, the mAs and the target/filter combination used for each view were also recorded. After, the entrance skin exposure was measured using an ion chamber (type 6-cc) with an electrometer. The exposure measured was then converted to MGD according to ACR recommendations. In this study, the estimated MGD per film was 1.42+0.80 mGy for CC views and 1.56 ±0.86 mGy for MLO views (with $p<0.001$). It was also found that 96.1 % of CC films and 94.2 % of MLO films had doses less than 3.0 mGy as

recommended by the ACR. a significant difference was found between MGD from CC views (1.42 ± 0.80) and MGD from MLO the MGD obtained per CC views and MLO views were respectively. They also conclude that the MGD per CC and MLO film was significantly related to CBT ($r = 0.610$, $p<0.01$ and $r = 0.596$, $p<0.01$ respectively).

In Thailand, Theerakul (2014) studied patient dose measurement in digital mammography. The purpose for the study was to determine the entrance skin exposure (ESE) and the MGD per exposure with grid for each projection of mammography service at King Chulalongkorn Memorial Hospital. The mammography equipment used for this study was a Selenia Dimensions, manufactured in 2009 by HologicLorad and verified by the department of medical science, Thailand in 2011. The study involved 200 patients. At the end of the study, the MGD was found to be 1.78 mGy for (RCC), 1.77 mGy for (LCC), 1.86 mGy for (RMLO) and 1.98 mGy for (LMLO) respectively. The average entrance skin exposure (ESE) was 6.79 mGy for (RCC), 6.83 mGy for (LCC), 7.15 mGy for (RMLO) and 7.83 mGy for (LMLO) respectively. The ESE and MGD from MLO views were greater than those from the CC views for the right and left sides because the MLO CBT is slightly thicker than the CC CBT. Overall, 91.41% of CC view and 89.14% of MLO view were lower than the reference level of 3.0 mGy. The MGD per image was significantly different between the CBT as classified by glandular content groups. It increased with increasing CBT, while decreasing with increasing age.

In 2011, Olivera et al, have done a study on image quality and dose in mammography in some continents. A total of 17 countries from Africa, Asia and

Eastern Europe including Malta and Greece, were involved in the survey, and the total of 54 mammography units were used ranging from 1 to 9 per country. The objective was to study mammography practice from an optimisation point of view by assessing the impact of simple and immediately implementable corrective actions on image quality. More than 21,000 mammography images were evaluated using a three-level image quality scoring system. Following initial assessment, appropriate corrective actions were implemented, and image quality was re-assessed in 24 units. The fraction of images that were considered acceptable without any remark in the first phase (before the implementation of corrective actions) was 70% for craniocaudal and mediolateral oblique projections, respectively. The main causes for poor image quality before corrective actions were related to film processing, damaged or scratched image receptors, or film-screen combinations that are not spectrally matched, inappropriate radiographic techniques and lack of training. Average glandular dose to a standard breast was 1.5 mGy (mean and range 0.59- 3.2 mGy). After optimisation the frequency of poor quality images decreased, but the relative contributions of the various causes remained similar. Image quality improvements following appropriate corrective actions were up to 50 percentage points in some facilities.

In Italy, Gisella et al, (2002) conducted a study on patient dose in full-field digital mammography. This study was carried out on four GE senographe 2000D digital mammography units, from January to May 2002.Two mammography units worked mainly in contrast mode, while the other two worked in standard mode. The main objective of this study was to compare performance and patient dose from fullfield digital mammography units in use clinically. Automatic Exposure Control stability

and the system linearity tests were performed on the four units. The tube output was also measured using an ionization chamber. The entrance air-kerma of 800 sampled craniocaudal views was calculated, as well as the average glandular dose.

At the end of the study, the linearity of the digital systems was very good, and the stability of the automatic exposure control was better than 5% for all systems. For the patient dose assessed, the two units that worked mainly in contrast mode have delivered 17% and 28% respectively, more dose compared to those that worked in standard mode. For the standard mode units, the mean average glandular dose was in the range of 1.25-1.37 mGy and 1.37-1.49 mGy for glandularity of 50% and 30% respectively. In conclusion, full-field digital mammography allows a significant clinical dose reduction compared to screen-film mammography units.

In Turkey, in 2002, Bor et al, have done a study on variations in breast doses for an automatic mammography unit. The purpose of the study was to assess variations of glandular doses for a group of patients when different dose modes are selected for a specific system. All measurements were obtained with a Senograph DMR mammography unit (GE Medical Systems). Automatic exposure control with either contrast or standard mode was routinely used in patient examinations. Entrance surface air kerma (ESAK) values were estimated from the post exposure mAs and from the recorded data. Subsequently the MGD for each view was calculated using the conversion factors assuming 50% glandular and 50% adipose tissue composition. At the end of the study, the average MGDs for the right craniocaudal (RCC) view for all beam qualities was 1.65 mGy, and 46.7 mm was the average compressed breast thickness for this view. Average MGDs were 1.61, 1.76, and 1.35 mGy respectively for Mo-Mo, Mo-Rh, and Rh-Rh anode filter selections, respectively. Conversely,

2.18 and 1.47 of breast doses were measured for contrast and standard dose modes at the most often used (Mo-Mo) anode filter selection.

In Ireland, a study was done by McCullagh et al, (2011) on clinical dose performance of full field digital mammography in a breast screening program. The aim of this study was to use the results from a clinical breast dose survey to examine the differences between three different FFDM models in terms of terms of exposures selection, breast MGD and AEC dose contribution. A total of 28 X-ray units (11 GE Essential, 10 Hologic Selenia, 7 Sectra MDM L30) encompassing a mixture of static and mobile settings were included in the survey. At the end of the study, the accuracy of the dose estimation was improved by inclusion of the AEC pre-exposure dose contribution. The photon- counting system demonstrated the lowest average MGD. The GE Healthcare and Hologic flat-panel detector systems demonstrated a small but statistically significant dose difference. The pre-exposure dose contribution did not exceed 13% of the total exposure dose for any system in the survey. A comparison of the system calculated organ dose estimate from each machine with the corresponding MGD calculated from medical physics measurements indicated reasonably accurate organ dose estimates for most systems in the survey.

In 2016 in Poland, Lusarczyk-Kacprzyk et al carried out a study on evaluation of dose and image quality in mammography with screen-film, CR and DR detectors. The objective for the study was to compare the quality of mammograms from several screen-film (SF), computed radiography (CR), and fully digital (DR) mammography systems using directly the ACR mammography accreditation phantom.

A number of 47 mammography units such as 26 Screen-films systems, 12 CR systems and 9 DR systems were involved in this study and Image quality and mean glandular doses were measured and compared for all the machines. The MGD was calculated using the breast simulated by 4.5 cm of PMMA with regards of the European guidelines for quality assurance in breast cancer screening and diagnosis. The visibility of the structures on the films (fibers, microcalcifications, and masses) was scored using the ACR mammography accreditation phantom.

As outcome found, the DR systems image quality was significantly higher than those from Screen-film and CR systems. Many Screen-film systems have failed for the image quality tests due to artifacts. All of the mammography units were within acceptable levels for MGD estimation. MGDs from CR systems were significantly higher than MGDs from both screen-film and DR systems.

The best image quality, at a reasonably low dose, was observed for the DR systems. The CR systems are capable of obtaining the same image quality as the SF systems, but only at a significantly higher dose. The ACR phantom can be routinely used to evaluate image quality for all types of mammographic systems.

Looking at the various works done by other authors, one will see that a lot of studies has been and is being done on digital mammography all over the world. However, it is evident that no such study has been done on mammography in BENIN. It is therefore very important to undertake this study to provide a baseline data for future research.

CHAPTER THREE

MATERIALS AND METHODS

3.0 Overview

In this chapter, materials and methodology used for this study are described. The selection criteria for the mammography equipment and patient data collection are also explained. It also highlights the challenges encountered during the data collection.

3.1 Materials

The materials used for this study are mammography machines, slabs of semi-circular polymethylmethacrylate (PMMA), a calibrated Piranha QC kit with Ocean software installed on a laptop, the ACR Mammography Accreditation Phantom, Leeds tests object TORMAS, a calliper, a ruler, a lawn ball tennis, a bathroom scale, a towel, Microsoft excel software and designed data sheets.

3.1.1 Mammography equipment

Three selected mammography systems were involved in this research: One computed radiography (CR) system at "Centre Autonome de Radiologie" (CAR) and another two screen-film (SF) systems at two different Hospitals: one private hospital: "Sainte ANNE D'AFRIQUE" (SAA) and one public Hospital: "Centre Hospitalier Universitaire Départemental Ouémé-Plateau" (CHD/OP) respectively from three different cities: Abomey-Calavi, Cotonou and Porto-Novo. The specifications of mammography equipment used are presented in Table 3.1.

Figures 3.1, 3.2 and 3.3 shows images of the mammography systems involved in the study.

Figure 3.1: Image of mammography system at Centre Autonome de Radiologie (CAR)

Figure 3.2: Image of mammography system at Centre Hospitalier Universitaire Départemental Ouémé Plateau (CHUD/OP)

Figure 3.3: Image of mammography system at Saint Anne d'Afrique (SAA)

Table 3.1: Specifications of mammography units selected

SPECIFICATIONS	FACILITIES		
	CAR	SAA	CHUD/OP
Type of Equipment	CR	SF	SF
Manufacturer	GENERAL ELECTRIC	SIEMENS	BMI BIOMEDICAL Int Sarl
Model	SENOGRAPH 700T	MAMOMAT C3	XM12
Serial number	33238CX7	01028S38	60G722
Year of make	Feb,2000	March, 1992	2008
Year of installation	Jan,2010	April,2013	2015
Mode of operation	Manual/AEC	Manual	Manual/AEC
Anode/filter combination (mm Al)	Mo/Mo	Mo/Mo	Mo/Mo
Focal-image distance (mm)	650	600	600
kVp range (Min-Max) (kV)	22-35	22-40	20-35
mAs range (Min-Max) (mAs)	4-600	2-500	1-640

3.1.2 Polymethylmethacrylate (PMMA)

Semi-circular slabs of polymethylmethacrylate (PMMA) commonly called Perspex were used in this study. Each slab has 100 mm of radius. A total of 8 slabs (6 have 10 mm thickness and 2 have 5 mm thickness) were used to mimic the breast. The PMMA is shown in figure 3.4 below.

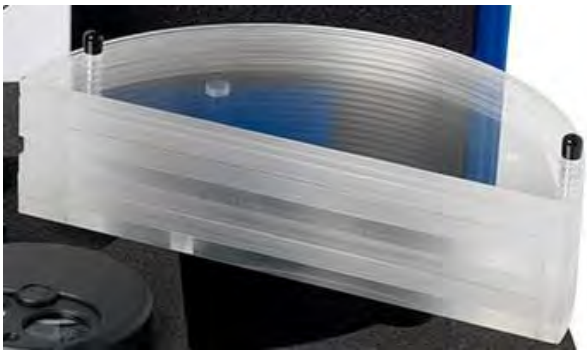

Figure 3.4: Image of PMMA slabs

3.1.3 Leeds test objects (TORMAS)

The Leeds tests object, TORMAS phantom was also used in this study for image quality evaluation. It has inside a ten-step step wedge, one high-contrast resolution patterns (1.0 to 20.0 lp/mm), a low-contrast resolution pattern, twelve low-contrast large details (5.6 mm diameter, decreasing thickness), 22 high-contrast small details (0.5 mm and 0.25 mm diameter, decreasing thickness, 11 details per each diameter), micro-particles representing micro-calcifications on a step wedge. Its picture is shown on Figure 3.5.

Figure 3.5: Image of leeds test object TORMAS (EFOMP Protocol, 2015)

3.1.4 The American College of Radiology Mammography Accreditation Phantom (ACR MAP)

The breast equivalent phantom used in this study for assessment of image quality was the ACR mammography accreditation phantom composed of following objects:

6 fibers with diameters of 1.56 mm, 1.12 mm, 0.89 mm, 0.75 mm, 054 mm, 0.40 mm

5 groups of simulated micro-calcifications with diameters of 0.54 mm, 0.40 mm, 0.32 mm, 0.24 mm, 0.16 mm.

5 masses thicknesses of 2.0 mm, 1.0 mm, 0.75 mm, 0.5 mm, 0.25 mm.

The ACR Mammography Accreditation Phantom is shown in Figure 3.6 below.

Figure 3.6: ACR Mammography Accreditation Phantom ("Phantom Mammo ACR Gammex 156 SimpliBuy,")

3.1.4 Piranha dosimeter

The dosimeter used for measurement in this study was the calibrated multi-electrometer Piranha model 657, coupled with a laptop via the Ocean software. Manufactured by RTI electronics AB, it was used to measure the kVp, HVL, Exposure or Entrance Surface Air Kerma (ESAK), exposure rate, exposure time measurements. The Ocean software allows to display the reading on the laptop and store the data on excel. The Piranha and the ocean software are shown in Figure 3.7.

Figure 3.7: Image of Piranha dosimeter with the Ocean software (www.rti.com)

3.2 METHOD

The data sheet in Appendix A1 was designed to collect useful equipment information from each selected facility. A data sheet in Appendix A2 was used to collect patient data from the three facilities. QC tests were carried out on the mammography systems to verify whether they were performing with internationally accepted criteria. The QC tests performed included: The unit assembly evaluation, kVp accuracy and repeatability, output repeatability and linearity, HVL and AEC performance, image quality tests and compression. mean glandular dose was estimated and compared with IAEA and European protocols values (EFOMP Protocol, 2015, IAEA, 2009)

3.2.1 Unit assembly evaluation

The objective of this test was to evaluate the mechanical functionality and assess the level of the equipment safety. A series of tests and verifications were conducted on the mammography equipment information recoded using in Appendix A3. The results obtained for this test are shown in Table 4.1.

3.2.2 kVp Accuracy

The objective of this test was to verify how accurate the kVp was. The detector (Piranha) was placed on the breast support, the sensitive area is placed at 50 mm from the chest wall, and laterally centred (reference point) and within the radiation beam and the compression applied shown in (Figure 3.8). Exposure parameters of 28 kVp (kVp_{set}) and 40 mAs (mAs_{set}) were selected to carry out five exposures in the manual mode. The measured kVp (kVp_{mea}) at each exposure were recorded on the data sheet Appendix B1. The parameters set are also recorded. The kVp accuracy

was then found out by calculating the percentage deviation of the measurements recorded, using equation (3.1). The result of this test is presented in Table 4.2.

$$\text{Deviation}(\%) = \frac{\text{kVp}_{\text{nom}} - \text{kVp}_{\text{mea}}}{\text{kVp}_{\text{nom}}} * 100 \qquad (3.1)$$

Where

Deviation (%) is the percentage deviation, kVp_{nom} is the selected on the machine, kVp_{mea} is the average of measured kVp value. This percentage deviation is considered as a measure of the accuracy and the acceptable range for accuracy is ±5% (IAEA, 2009).

3.2.3 kVp Repeatability

The objective of this test was to verify the repeatability of the kVp. For this test, two exposures were made firstly in the manual mode at a nominal kVp of 28 kVp and mAs of 40 mAs, with the detector positioned at the reference point. The measured kVp (kVp_{mea}), the set kVp (kVp_{nom}) and mAs (mAs_{set}) were recorded on a data sheet in Appendix B1. The two kVp_{mea} were used to calculate the percentage difference using the formula (3.2). Figure 3.8 represents the setup.

$$\text{Percentage Difference}(\%) = \frac{\text{kVp}_{\text{mea}}\text{maximum} - \text{kVp}_{\text{mea}}\text{minimum}}{\text{kVp}_{\text{mea}}\text{minimum}} \qquad (3.2)$$

Where: kVp_{mea} maximum is the measured kVp having the high value and kVp_{mea} minimum the measured kVp having the low value. For an acceptable kVp, repeatability percentage difference must be ≤ 5%.

For the accuracy of the results, three additional exposures were made using the same parameters set for the two previous exposure. A total of five kVp_{mea} were then recorded using the data sheet in Appendix B1 and the coefficient of variance of the five measured kVp was calculated according to the IAEA protocol (IAEA, 2009) using the formula (3.3).

$$\text{Coefficient of Variance (\%)} = \frac{SD}{\bar{x}} * 100 \qquad (3.3)$$

Where: SD is the Standard Deviation calculated over measured kVp, and $\bar{x}$ is the average of the measured kVp. For acceptable kVp repeatability the Coefficient of variance (%) should be within the range of ≤ 2% (IAEA, 2009)

3.2.4 Output Repeatability and linearity

The objective of this test was to evaluate the repeatability and the linearity of the air kerma for a given mAs and to estimate the normalized output value (µGy/mAs at 1 m). The dosimeter setup was the same as that used for kVp accuracy and repeatability (Figure 3.8). The distance between the focal spot and the dosimeter surface was recoded on the data sheet Appendix B2. The manual exposure mode was selected as well as the Mo/Mo target/filter combination and the tube voltage was fixed at 28 kVp. Three different values of mAs such as 40 mAs, 80 mAs and 125 mAs were selected among the range of mAs values normally used clinically. For each value of mAs selected two exposures were taken and the measured air kerma was recorded on the data sheet.

The output repeatability was evaluated by calculating the percentage Difference of the two air kerma measured for a given value of mAs, using the equation (3.2). (IAEA, 2009). The results of this test were presented in Table 4.2.

For output linearity (L), the average value of the obtained readings of air kerma was calculated for each corresponding mAs selected. The output (y) then derived by dividing each average measured air kerma by the corresponding mAs and the results were recorded on a data sheet in Appendix B2. The output linearity was then calculated using equation (3.4). The result of this test is presented in Table 4.2

$$L\,(\%) = 100 * \frac{(y_1 - y_2)}{(y_1 + y_2)} \qquad (3.4)$$

Where:

y_1 and y_2 are the output values obtained at a consecutive mAs value by dividing each average air kerma value by the corresponding mAs. The acceptable linearity of output must be less than 10%.

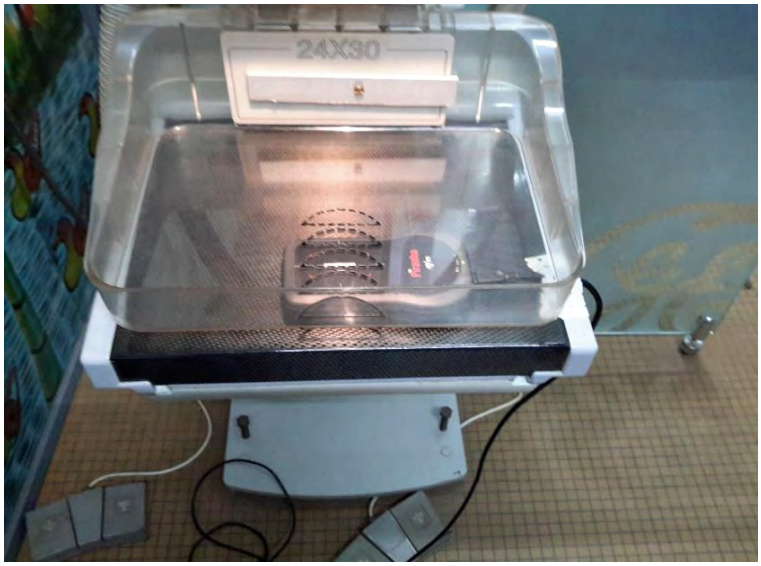

Figure 3.8: Setup of kVp accuracy, repeatability and output repeatability, linearity

3.2.5 Normalized Output

The objective of this test was to confirm that the output at 1m within the standards range (< 30μGy/mAs at 1m). Inverse square law correction was applied to the average value of output calculated previously for the different mAs to obtain a normalized output at the distance of 1m from the focal spot. The response was converted in μGy/mAs and was recorded on the data sheet in Appendix B2. The result of this test is presented in Table 4.2.

3.2.6 Half Value Layer (HVL)

This test aimed to confirm that the total filtration of the X-ray beam met the minimum requirements of the international standards (IAEA, 2009). This measurement was done in the manual mode at 28 kVp and 40 mAs. The sensitive volume of the dosimeter was placed at 50 mm from the chest wall, laterally centred. It remained completely in the collimated radiation field. The compression paddle was also applied. Four, five and six exposures were carried out at facility SAA, CAR and CHUD/OP respectively according to the clinical exposure factors (kVp_{set}, mAs_{set}) range available in each facility. The readings such as measured kVp (kVp_{mea}) and measured (HVL_{mea}) were recorded on a data sheet in Appendix B3. Verification was then made to confirm whether the total filtration of each machine was within the international standards range required by IAEA using the equation (3.5). The result of this test is presented in Table 4.2

$$\frac{kVp_{mea}}{100} + 0.03 \leq HVL_{mea} \leq \frac{kVp_{mea}}{100} + C \qquad (3.5)$$

Where: kVp_{mea} was the measured value for the nominal kVp selected and HVL_{mea} was the measured filtration 0.03 is a factor that compensates for the thickness of the compression plate and C was a factor that compensates for the anode/ filter combination used. (IAEA, 2011).

Note: C = 0.12 for M_O/M_O, C = 0.19 for M_O/Rh, C = 0.22 for Rh/Rh, C = 0.30 for W/Rh,

3.2.7 Automatic Exposure Control

The objective of this test was to assess the repeatability of the AEC. This was done by making five exposures of 45 mm PMMA slabs in the automatic mode, the displayed mAs (mAs_{dis}) were recorded on the data sheet presented in Appendix B4. The AEC repeatability was estimated by finding the coefficient of variance of the mAs displayed using equation 3.3. The result of this test is shown in Table 4.2. Comparison was made with IAEA standards values (IAEA, 2009).

3.3 Compression tests

The objective of this test was to check that the mammography units provided an adequate and uniform breast compression in both manual and automatic mode. To assess the accuracy of the compression force indicator when it is present on the equipment. It was also to check the accuracy of the compression thickness indicator.

3.3.1 Compression alignment measurement

A bath towel was placed on the breast support to protect it. A lawn tennis ball was placed at the central point of the breast support and was compressed with the maximum possible compression force shown in Figure 3.9. The distance between the

compression paddle and the breast support was measured at each angle of the breast support using a calliper. Information was recorded using the data sheet in Appendix B5. The percentage difference from the average of measurements from the right side and the left side of the Bucky was calculated and compared to the IAEA standards (IAEA, 2009). The result of this test is shown in Table 4.2.

Figure 3.9: Setup of compression paddle alignment test

3.3.2 Compression force

3.3.2.1 Automatic compression

On the towel already placed on the breast support to protect it from scratch, a bathroom scale was placed and centred. A tennis ball was then placed and centred on the bathroom scale (Figure 3.10). The automatic compression was used to compress the tennis ball and the reading (R) value from the bathroom scale was recorded on the data sheet in Appendix B6. The compression was released after reading. The compression force was then calculated using the formula (3.6) and compared to IAEA standard values. The result of test is presented in Table 4.2.

3.3.2.2 Manual compression

The setup used for the automatic compression was kept. The compression paddle was manually moved to compress the tennis with the maximum possible compression level. The reading (R) from the bathroom scale was recorded using Appendix B6, compression was released after reading, compression force was calculated using the formula (3.6) and compared to IAEA standard values. The result of this test is presented in Table 4.2.

$$\text{COMPRESSION FORCE (N)} = \text{R(kG)} * 10(\text{N/kG}) \quad (3.6)$$

Figure 3.10: Setup of compression force test

3.3.3 Compression thickness indicators

Semi-circular PMMA slabs were used to mimic the thickness of compressed breast. Three different thicknesses (20 mm, 45 mm and 70 mm) of PMMA were placed on the breast support and compressed with minimum compression force recorded from each machine (Figure 3.11). The distance between the compression paddle and the breast support were measured for the system that did not have compression indicator

and both information were recorded. The displayed thicknesses (Tk_{dis}) indicated on the system were then compared to the set thicknesses (Tk_{set}). Where there is no thickness indicator on the system, the measured thicknesses (Tk_{mea}) were compared to the set thickness of PMMA slabs. All of the information were recorded using the data sheet in Appendix B5. Deviations were then calculated using equation (3.1) and compared to the IAEA standards. The result of this is presented in Table 4.2.

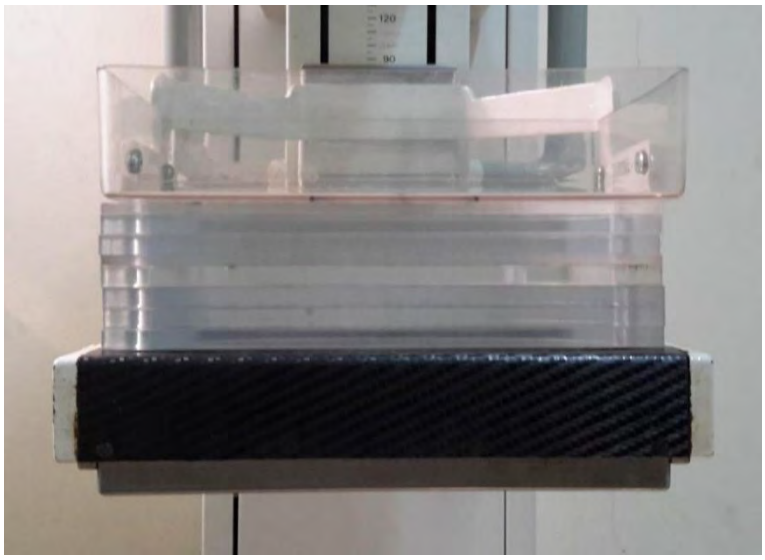

Figure 3.11: Setup of compression thickness test

3.3.4 Image quality

3.3.4.1 Image quality evaluation

The objective of this test was to ensure that mammograms produced by the system have acceptable optical density, contrast and quality.

The ACR Mammography Accreditation Phantom was then placed on the breast support and aligned with the chest wall and laterally centred (Figure 3.12). The compression plate was lowered until to touch the phantom. The loaded cassette with appropriate film was placed in the Bucky and an exposure was made using the technical parameters clinically used in mammography practice. The film was

processed using the film processor normally used in the facility. For image quality assessment, the film was viewed on viewing box and subjective analysis was done following the IAEA protocol (IAEA, 2009). The result of this test is presented in Table 4.3. The results obtained were compared to international standards values.

3.3.4.2 Spatial resolution test

The objective of this test was to determine the system high contrast resolution. To verify whether the mammography system can find separately two micro-calcifications. A mammography Leeds object test was positioned on the Bucky aligned with the chest wall and laterally centred (Figure 3.13). A loaded cassette was placed on the Bucky and compression was applied. An exposure was made, and the film processed in similar clinical practice condition. The subjective analysis was used to score the film using a viewing box and magnifier lens. The results are presented in Table 4.3.

Figure 3.12: Setup of image quality test

Figure 3.13: Setup of resolution test

3.4 Mean Glandular Dose (MGD) Estimation

This test objective was to estimate the dose delivered to the glandular tissues within the breast. It is called mean glandular dose. The MGD was calculated from the Entrance Surface Air Kerma (ESAK) without backscatter measured at a given focus-entrance surface distance which was converted to MGD using the formula (2.1). This test was done through two steps: phantom MGD estimation and patient MGD estimation.

3.4.1 Phantom MGD estimation

A calibrated dosimeter (Piranha) was positioned at the reference point (50 cm from the chest wall edge and laterally centred) on the breast support. The PMMA slab of 30mm was also placed at one side of the dosimeter to mimic the Compressed Breast thickness (CBT) and the compression was applied (Figure 3.14). The exposure parameters such as kVp, mAs, anode/filter combination was selected in respect of the PMMA thickness. The distance focus-dosimeter named D_1 was measured. The distance focus-surface of PMMA named D_2 was calculated ($D_2 = D_1 - CBT$. The same procedure was performed for each PMMA thickness of 40 mm, 45 mm, 50 mm, 60 mm and 70 mm.

Since the surface of the dosimeter and that of the PMMA slabs were not at the same height when measurement was performing. The $ESAK_i$ measured at the dosimeter surface was first corrected to the surface of each PMMA slabs used to mimic the breast. This was done using the inverse square law equation given in equation (3.7)

$$ESAK = ESAK_i * \frac{D_1^2}{D_2^2} \qquad (3.7)$$

Where: $ESAK_i$ is the one measured at the surface the dosimeter, ESAK is the entrance surface air kerma at the surface of the PMMA with a given thickness. D_1 is the focus-dosimeter distance, and D_2 is the focus-PMMA slabs surface distance.

This allowed to determine the Entrance Surface Air Kerma named ESAK at the surface of each PMMA thickness. The MGD for each PMMA thickness was calculated using equation (2.1). Exposure parameters (kVp, mAs, target/filter combination), T $ESAK_i$, ESAK, D_1, D_2 and MGD were recorded using the data sheet in Appendix B8.

Another exposure was made using the AEC mode (semi AEC mode from CAR system and full AEC mode from CHUD/OP system) and following the same procedure as above. Information was recorded on data sheet in Appendix B9. The results of the manual mode and the AEC mode are shown in Table 4.4 and Table 4.5 respectively. The results obtained were compared to IAEA (2011) standards.

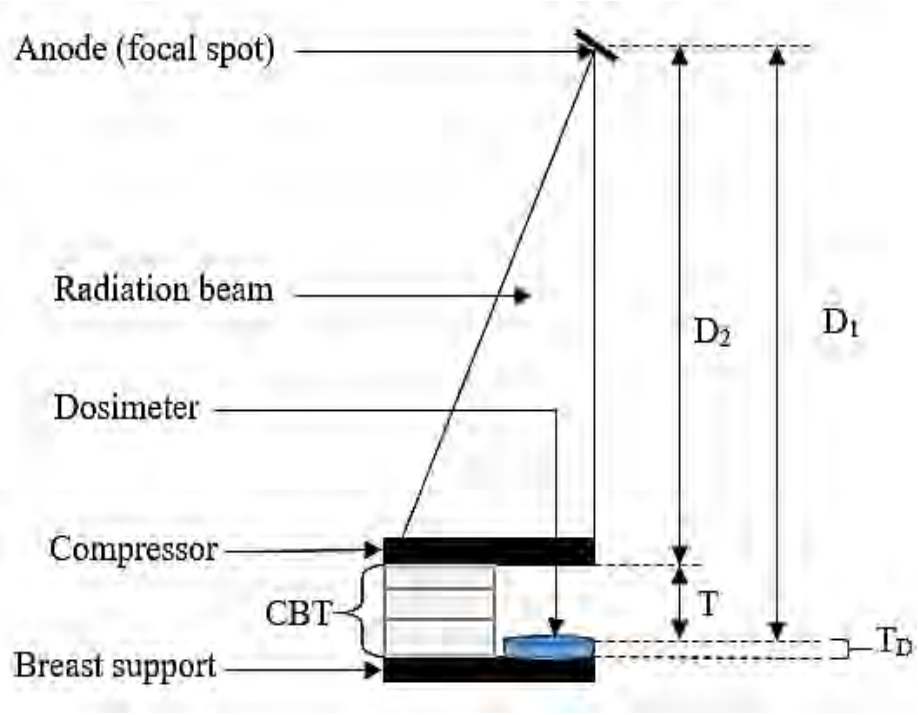

FIG 3.14: Setup of ESAK measurement

D1 is the distance from the focal spot to the surface of the dosimeter, D2 is the distance from the focal spot to the surface the compressed breast, TD represents the dosimeter thickness; T is the distance between the dosimeter surface to the compressed breast surface. $T = CBT - T_D$ and $D_2 = D_1 - T$.

3.4.2 Patient MGD estimation

A total of 28 patients undergoing mammography examination and from whom approval was got, were involved in this study only at the CHUD/OP facility. Patients data age, CBT from Right Craniocaudal (RCC) and Left Craniocaudal (LCC) views, kVp, mAs, Target /filter combination were recoded using the data sheet in Appendix A2.

To get the ESAK of each patient, the normalized output of the system from phantom measurement. The output was then calculated for each PMMA thickness using equation 3.9.

$$\text{Output}(mGy/mAs) = \frac{\text{ESAK (mGy)}}{\text{mAs}} \qquad (3.9)$$

Where: the mAs can be the selected mAs_{set} in manual mode or displayed mAs_{dis} in AEC mode.

A graph from calculated output values against selected kVp (kVp_{set} for manual mode) or displayed kVp (kVp_{dis} for AEC mode) from each PMMA exposure was plotted and it shows in Figure 4.2. Then a linear equation presented by equation (3.10) was generated from the plotted graph (Akrobortu et al, 2013).

$$\text{output}\ (mGy/mAs) = \text{akVp (kV)} + \text{b} \qquad (3.10)$$

Where: y corresponds to output (mGy/mAs) and x corresponds to kVp. The a is the equation coefficient while b is the constant. A graph of kVp and output against compressed breast thickness was plotted and it is presented in Figure 4.3.

The ESAK for both RCC and LCC views was then calculated by multiplying the Output (mGy/mAs) by the recorded mAs. This gave the ESAK in mGy corresponding to each patient CBT using equation (3.11).

$$ESAK = Output * mAs\ (recorded) \qquad (3.11)$$

The MGD corresponding to each CBT from RCC and LCC views according to each patient age range, were then calculated using equation (2.1). The conversion factors g, c, s, used for this study were interpolated or extrapolated from Dance et al (2000, 2009, and 2011). The result of this test is presented in Table 4.9 and Table 4.10.

The mean, standard deviation, range of MGD were calculated. Finally, results were also compared to the IAEA and European protocol standard MGDs.

CHAPTER FOUR

RESULTS AND DISCUSSIONS

4.0 Overview

It is presented in this chapter the results obtained from data analysis. It is described and discussed the various results of QC tests, MGD estimated from phantom measurement as well as from patients. The results from kVp accuracy and repeatability, half-value layer, output repeatability and linearity, and the automatic exposure control repeatability are also presented.

4.1 Quality Control assessment

Table 4.1, shows the results of the three mammography unit assembly evaluations.

Table 4.1: Mammography unit assembly assessment

PARAMETER	FACILITIES		
	SAA	CAR	CHUD/OP
Mechanical stability of free-standing unit	pass	pass	pass
Lights indicator	Fail	pass	pass
Units motion function	pass	pass	pass
Locks and detents function	pass	pass	pass
Angulation indicators	pass	pass	pass
Wobble and vibration	pass	pass	pass
Image receptors sliding and holding during gantry angulation	pass	pass	pass
Compression paddle condition	pass	pass	pass
Automatic compression release	Fail	pass	pass
Operator shielding evaluation	pass	pass	pass
Safety of patient/operator against units	pass	pass	pass
Availability of technique parameters chart	Fail	Fail	Fail

Table 4.1shows that the majority of the unit assembly evaluation was successful. Except at facility SSA where the light field indicator and the automatic compression

release after exposure failed. The exposure parameters chart was not available for all facilities.

Table 4.2, below presents the results of the QC assessment performed on the machines such as kVp accuracy and repeatability, output repeatability and linearity, HVL, compression (alignment, force and thickness) AEC repeatability.

Table 4.2: Mammography systems performance assessment

QUALITY CONTROL TESTS (Acceptable ran)	**RESULTS**			**OBSERVATION**
	SAA	**CAR**	**CHUD/OP**	**Pass / Fail**
kVp accuracy DEV(%) (± 5%)	0.4	-3.6	-4.1	Pass
kVp repeatability COV (%) ≤ 2%	0.1	1.83	0.12	Pass
HVL (mmAl) (kVp/100+0,03≤HVL≤kVp/100+c	0.32	0.35	0.32	Pass
Output repeatability (COV (%) ≤ 5/%	0.074	0.08	0.24	Pass
Output linearity (L (%) < 10%	0.013	-0.05	0.9	Pass
Normalyzed output (µGy/mAs at 1m) >30µG/mAs	48.05	32.18	34.18	Pass
AEC repeatability COV (%) ≤ 5%	-	2.3	2.45	Pass
Compression alignment	3.89	3.19	4.05	Pass
Compression thickness	-5	-5	-2.5	Pass
Compression force : M/A (≤300N/ [150 N-200 N]	120/100	140/130	None/170	Faill/fail/Pass

The kVp accuracy and repeatability for SAA was 0.4% and 0.1% respectively, for CAR it was -3.6% and 1.8% respectively, and for CHUD/OP it was -4.1% and 0.12% respectively. The results from the Table 4.2 fell within the acceptable range.

This means for all machines, the percentage difference between the kVp set on the machine and the kVp measured is within the acceptable limits.

The HVL measured was 0.32 mm Al for SAA, 0.35 mm Al for CAR and 0.32 mm Al for CHUD/OP which agreed with IAEA standards values which means the radiation beam quality is correct and the total filtration is working perfectly.

The output repeatability and linearity were 0.074% and 0.013% while the normalized output at 1m was 48.30 µGy/mAs for SAA. The output reputability and linearity were 0.08% and -0.05% while normalized output at 1 m was 32.18 µGy/mAs for CAR and 0.24% and 0.9% while normalized output à 1 m was 34.18 µGy/mAs for CHUD/OP. The meaning is that the air kerma repeatable and constant for any given mAs.

The AEC repeatability from CAR 2.3% and 2.45% from CHUD/OP, have also fallen within the acceptable range. The meaning is that the AEC mode is able to produce suitable image contrast and keep as low as possible the MGD. For the compression tests such as alignment and thickness have been scored correctly by all of the systems while the SAA and CAR have net passed the test of compression force. The score of 100 N and 130 N obtained for power compression respectively by SAA and CAR was below the standards levels [150 N – 200 N] while CHUD/OP have passed the test of the power compression with 170 N, but it does not have the manual compression. For the manual compression SAA and CAR recorded respectively 120 N and 140 N which were also lesser than the standards values [200 N-300 N]. This means the compression provided is not adequate for SAA and CAR.

4.2 Image quality tests

Table 4.3 is shows the results from subjective analysis (human analysis) tests upon the ACR mammography accreditation phantom and the leeds test objects TORMAX

Table 4.3: Image quality tests results

Tests		Scores per facilities		
		SAA	CAR	CHUD/OP
ACR accreditation Phantom test	Fibers (tolerance ≥ 4) *	4	5	4
	Microcalcifications (tolerance ≥ 3) *	3	4	4
	Mass (tolerance ≥ 3) *	3	5	4
Spatial resolution tests	Lines pairs/mm (Tolerance ≥ 11lp/mm) *	13	18	15

*(IAEA, 2009)

The results of the image quality evaluation were satisfactory as it can be seen in the Table 4.3 above where SAA have got 4 fibers, 3 micro-calcifications and 3 masses for the ACR Accreditation phantom test and 13 lines pairs/ mm for the spatial resolution test. The facility CAR machine scored for the ACR test, 5 fibers, 4 micro-calcifications groups and 5 masses while the test spatial resolution was 18lines pairs/mm. The CHUD/OP system recorded a score of 4 fibers, 4 groups of micro-calcification and 4 masses while from the spatial resolution it has got 15 lines pairs/mm. Therefore, all the mammography systems passed the subjective image quality evaluation their score fall within the acceptable range which was for ACR phantom (≥ 4 for fibers; ≥ 3 for micro-calcifications and ≥ 3 for masses) and the spatial resolution test that was 11 lp/mm for acceptable limits and 15 lp/ mm for the

achievable limit. This means all the systems selected have ability to detect breast lesions and differentiate them from normal tissues.

4.3 Estimation of Mean Glandular Dose

4.3.1 Phantom MGD measurement

Table 4.4 represents the summary of the entrance surface air kerma and output calculated at the surface of each simulated compressed breast thickness using the PMMA phantom with various thicknesses of slabs.

Table 4.4: Summary of ESAK and Output from each mammography system

PMMA	SAA		CAR		CHUD/OP	
Thickness	ESAK (mGy)	Output (mGy/mAs)	ESAK (mGy)	Output (mGy/mAs)	ESAK (mGy)	Output (mGy/mAs)
30.00	3.53	0.10	3.18	0.06	6.09	0.14
40.00	4.15	0.11	5.28	0.09	8.31	0.14
45.00	5.40	0.13	6.67	0.10	10.80	0.18
50.00	6.81	0.14	6.79	0.10	8.79	0.15
60.00	7.97	0.14	9.82	0.11	9.15	0.16
70.00	9.18	0.14	12.89	0.11	12.97	0.20

Table 4.4, shows that ESAK and output increase as the compressed breast thickness increases. The maximum value of ESAK was recorded from the highest breast thickness for all mammography units. The maximum values of 9.18, 12.89 and 12.97 mGy were obtained from SAA, CAR and CHUD/OP respectively.

Table 4.5 represents the summary of estimated MGD from selected mammography systems at each facility.

Table 4.5: Summary of calculated MGD from each facility compared to IAEA Standards

CBTPMMA (mm)	FACILITIES						IAEA STANDARDS (mGy)*
	SAA		CAR		CHUD/OP		
	MGD (mGy)	MGD_{AEC} (mGy)	MGD (mGy)	MGD_{AEC} (mGy)	MGD (mGy)	MGD_{AEC} (mGy)	
30	0.99	-	0.92	1.05	1.51	0.45	1.5
40	0.91	-	1.24	0.82	1.80	0.35	2
45	1.07	-	1.39	0.74	1.84	0.30	2.5
50	1.24	-	1.27	0.52	2.02	0.28	3
60	1.20	-	1.55	0.45	2.08	0.24	4.5
70	1.16	-	1.71	0.47	2.45	0.21	6.5

*(IAEA HHS No.2, 2011)

Table 4.5 shows the calculated MGD corresponding to each specific PMMA CBT. From facility SAA, mean MGD was 1.09 mGy (from 0.91 to 1.24 mGy). The AEC mode was not available on this machine. From facility CAR, mean MGD was 1.35 mGy (from 0.92 to 1.71 mGy) and 0.67 mGy (from 0.45 to 1.05 mGy) for manual and AEC mode respectively. From facility CHUD/OP, mean MGD was 1.95 mGy (from 1.51 to 2.45 mGy) and 0.30 mGy (from 0.21 to 0.45 mGy) for manual and AEC mode respectively. All MGDs calculated were within the standards limits. This means the selected machines were not overexposing patients.

Figure 4.1 shows the graph of output variation against tube voltage of the mammography units at CHUD/OP and the equation generated from it was $y = 0.0265x - 0.669$ which was used to generate Table 4.6.

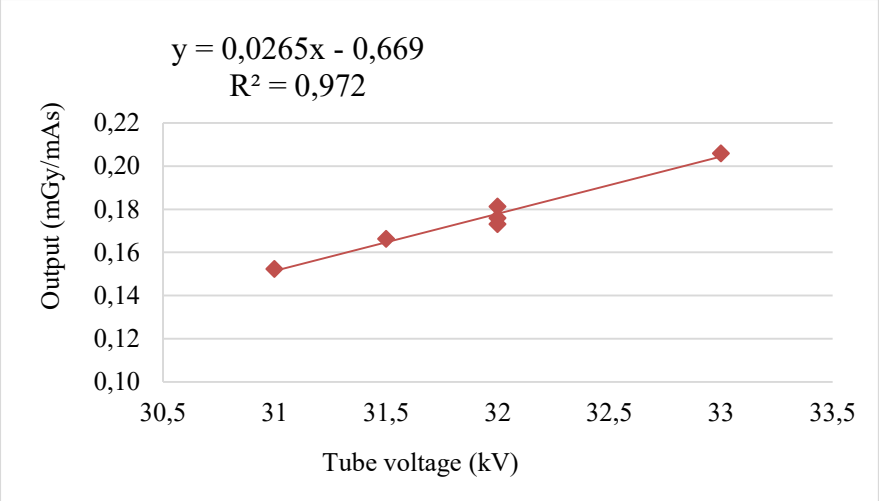

Figure 4.1: A graph of calculated output (mGy/mAs) against tube voltage (kV) from mammography system CHUD/OP

Figures 4.2 and 4.3 below represent the graphs of comparison of the kVp under the manual and kVp under AEC mode against CBT at CHUD/OP and CAR respectively

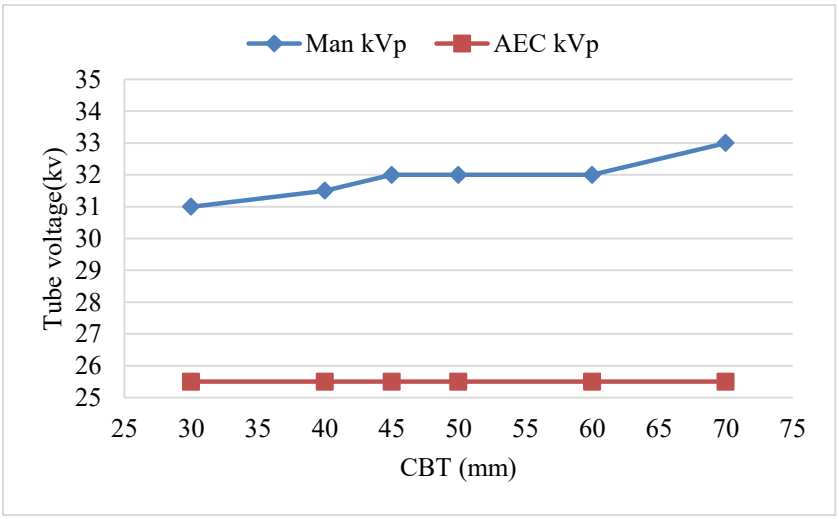

Figure 4.2: Comparison of kVp (manual mode) and kVp (AEC mode) against CBT for CHUD/OP

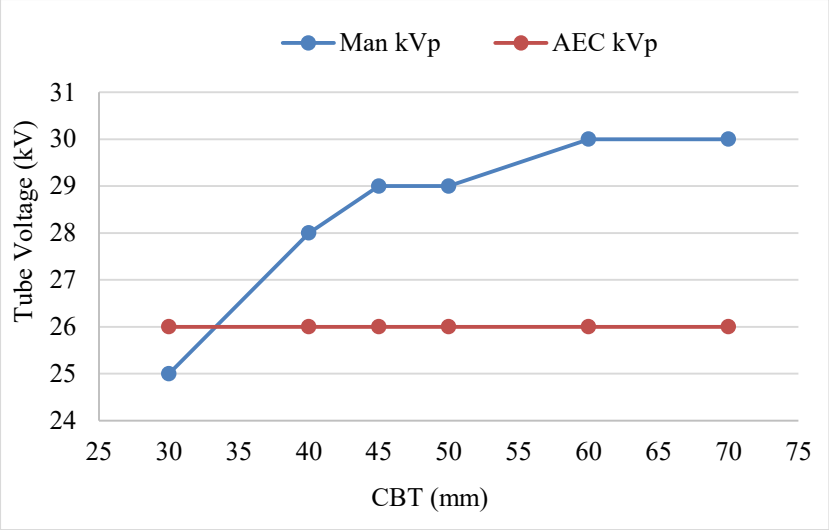

Figure 4.3: Comparison of kVp (manual mode) and kVp (AEC mode) for CAR

The kVp selected using manual mode was increased from 31 kV to 33 kV for CHUD/OP (Figure 4.2) and from 25 kV to 30 kV for CAR (Figure 4.3) respectively when increasing the CBT on other hand displayed kVp under AEC mode were constant at 25.5 kV for CHUD/OP and 26 kV for CAR respectively, over the range of CBT. The kVps under manual mode were higher than those under AEC for the two facilities. The result from figures 4.2 and 4.3 indicate the AEC mode compensates for the kVp when the breast thickness was increased.

Figures 4.4 and 4.5 are graphs of mAs selected using the manual mode and mAs displayed under the AEC mode against CBT for CHUD/OP and CAR respectively.

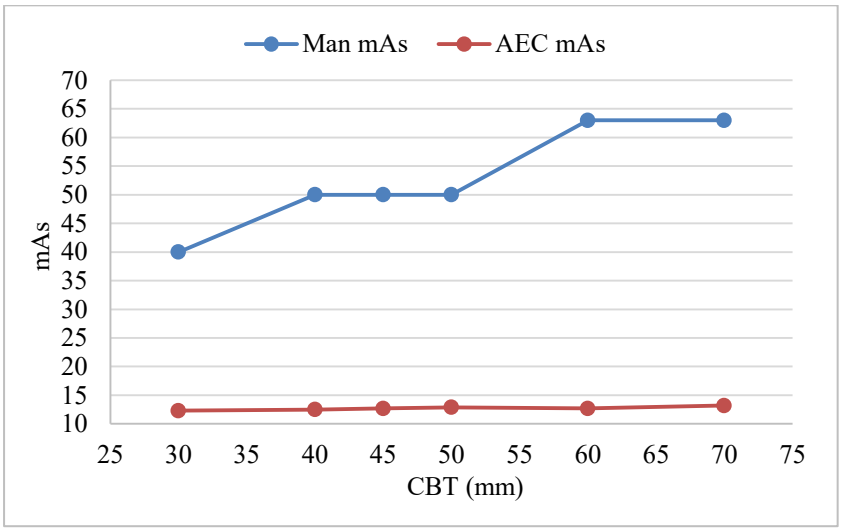

Figure 4.4: Graph of comparison of mAs (manual mode) and (AEC mode) for CHUD/OP.

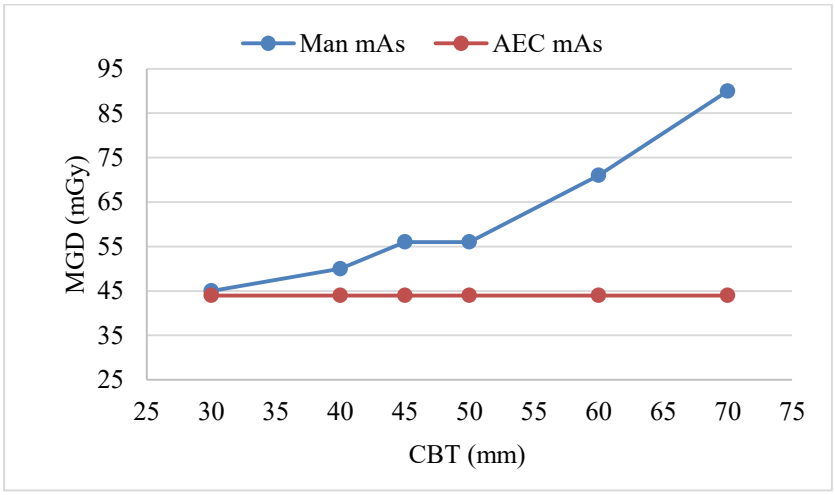

Figure 4.5: Graph of comparison of mAs (manual mode) and mAs (AEC mode) for CAR

Figures 4.4 and 4.5 show that mAs under manual mode increases from 40 mAs to 63 mAs for CHUD/OP and from 45 mAs to 90 mAs for CAR when the breast thickness increases. However, the mAs under AEC was constant at 44 mAs for CHUD/OP and

varied from 12.3 mAs to 13.1 mAs for CAR, after increasing the breast thickness. This means that the AEC mode compensates for mAs when increasing the CBT.

Figures 4.6 and 4.7 are the graphs showing the comparison of variation of the MGD under manual mode and MGD under AEC mode against CBT for CHUD/OP and CAR respectively.

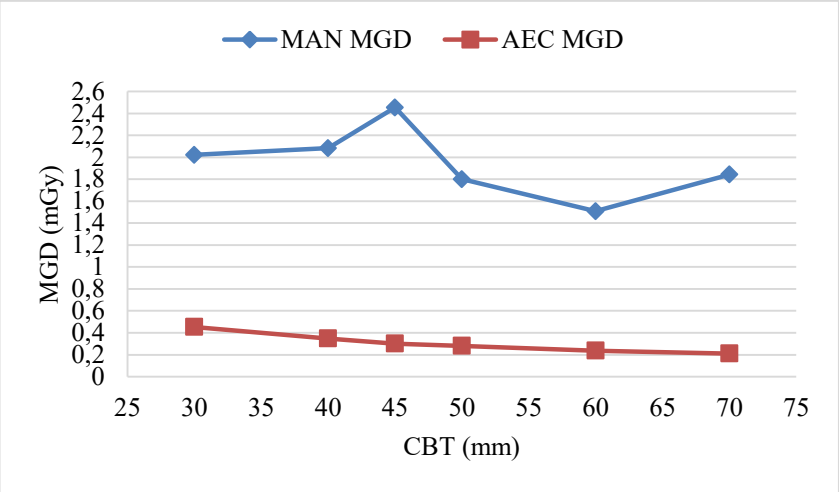

Figure 4.6: Comparison of estimated MGD (AEC mode) and MGD (Manual mode) for CHUD/OP.

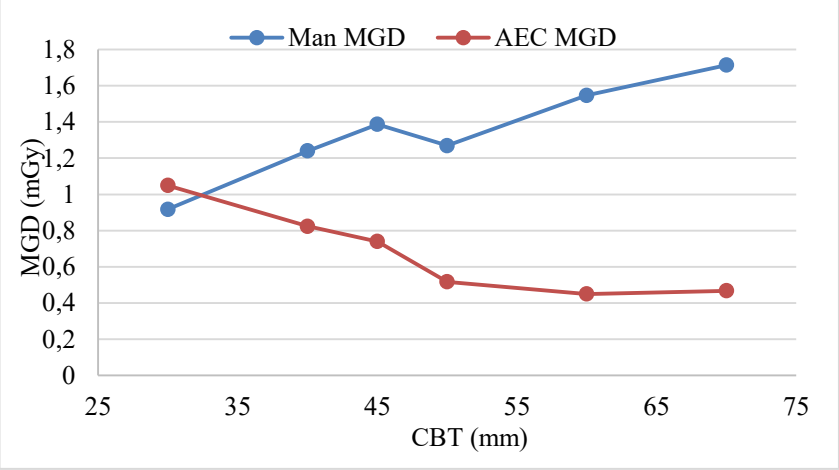

Figure 4.7: Comparison of estimated MGD (AEC mode) and (Manual mode) for CAR.

Figures 4.6 and 4.7 above shows that the mean MGDs obtained under AEC were 0.3 mGy for CAR (from 0.47 mGy to 1.05 mGy) and 0.35 mGy (from 0.21 mGy to 0.45

mGy) for CHUD/OP while the mean MGDs obtained under the manual mode were 1.35 mGy (from 0.92 mGy to 1.71 mGy) for CAR and 1.64 mGy (from 1.84 mGy to 2.02 mGy) for CHUD/OP. The MGDs obtained under AEC mode were lower than the MGD obtained under manual mode. The difference of MGD between the two modes was around 1.05 mGy at CAR and 1.31 mGy at CHUD/OP. It can then be deduced from the results obtained that breasts were receiving more dose from manual exposure mode than automatic exposure control mode.

4.3.2 Patients MGD estimation

A total 21 out of 28 patients undergoing mammography examination at the facility CHUD/OP participated in this study. After approval from each patient data such as kVp, mAs, CBT, age, type of examination, numbers of examination views were collected

Table 4.6: Summary of patient data collected at CHUD/OP

Age	Type of exam	Anode/ filter	kVp (kV)		mAs(mAs)		CBT (mm)	
			RCC	LCC	RCC	LCC	RCC	LCC
63	Diagnostic	Mo/Mo	32	32	50	50	51	50.6
40	Diagnostic	Mo/Mo	29	29	32	32	35	34
54	Diagnostic	Mo/Mo	32	32	50	50	45	45
50	Diagnostic	Mo/Mo	32.5	32.5	50	50	51	50
41	Diagnostic	Mo/Mo	28	28	25	25	25	24
53	Screening	Mo/Mo	33	32	30	30	20	18.7
45	Diagnostic	Mo/Mo	32	32	50	50	55	50
42	Diagnostic	Mo/Mo	29	29	32	32	25	24
63	Diagnostic	Mo/Mo	31	31	40	40	48	47
46	Diagnostic	Mo/Mo	33	33	80	80	68	65
42	Screening	Mo/Mo	34	34	63	63	60	59
51	Diagnostic	Mo/Mo	32	32	50	50	49	48
40	Screening	Mo/Mo	32	32	40	40	50	50
61	Diagnostic	Mo/Mo	30	30	40	40	45	44
40	Diagnostic	Mo/Mo	32.5	32.5	40	40	48	48
44	Diagnostic	Mo/Mo	33	33	40	40	59	60
54	Screening	Mo/Mo	33	33	32	32	35	36
43	Diagnostic	Mo/Mo	33	33	40	40	50	51
64	Diagnostic	Mo/Mo	35	35	50	50	60	62
63	Diagnostic	Mo/Mo	33	33	50	50	65	65
58	Diagnostic	Mo/Mo	35	35	40	40	55	54
28	Screening	Mo/Mo	30	30	40	40	45	45
32	Screening	Mo/Mo	32	32	50	50	55	55
71	Diagnostic	Mo/Mo	28	28	25	25	24	25
68	Diagnostic	Mo/Mo	29	29	32	32	35	35
25	Diagnostic	Mo/Mo	34	34	63	63	58	60
35	Screening	Mo/Mo	33	33	62	62	59	58
70	Diagnostic	Mo/Mo	30	30	35	35	30	30

From Table 4.6 above, 28 patients were recorded with a minimum of 25 years and the maximum of 71 years. The mammography unit uses in clinical practice a Mo/Mo anode/filter combination. The range of kVp used in clinical conditions was from 28 kV to 35 kV while the mAs was from 25 mAs to 80 mAs. A total of 21 diagnostic mammography procedures were performed whiles 7 screening mammography procedures were performed. A minimum number of three views were taken per breast and then minimum of 6 views per patient. A total of 168 views were taken. This research was only focus on data concerning Craniocaudal views (CC) therefore a total 56 CC views were taken with 28 RCC views and 28 LCC views. The CBT varies from 18.7 mm to 68 mm.

The kVp collected from patient data was introduced into the equation (3.10) to derive the output of each kVp

$$Output = a\,kVp + b \qquad (3.10)$$

The y-axis corresponds to output values and x-axis corresponds to the tube voltage values. The values a and b were obtained from the equation generated from Figure (4.1.) where a = 0.0265 and b = - 0.665.

Table 4.5 summarizes the output generated from each breast thickness against the kVp.

The Table 4.7 represents the variation of the output against the tube voltage selected for patient's exposure**.**

Table 4.7: Variation of Output against kVp at CHUD/OP

kVp (kV)		Output (mGy/mAs)	
RCC	**LCC**	**RCC**	**LCC**
28	28	0.07	0.07
29	29	0.1	0.1
30	30	0.13	0.13
31	31	0.15	0.15
32	32	0.18	0.18
32.5	32.5	0.19	0.19
33	32	0.21	0.18
33	33	0.21	0.21
34	34	0.23	0.23
35	35	0.26	0.26

It shows that the output is strongly related to the tube voltage. So, an increase in the kVp leads in the increase in output.

Table 4.7, shows how the selected technique factors from operator (manual mode) and the mean glandular dose per projection views vary when the breast thickness varies for patient age range of [40 - 49].

Table 4.8: Variation of MGD, kVp, mAs against CBT for patient age [40 - 49].

Age Range [40 - 49]							
CBT (mm)		**kVp (kV)**		**mAs (mAs)**		**MGD (mGy)**	
RCC	**LCC**	**RCC**	**LCC**	**RCC**	**LCC**	**RCC**	**LCC**
25	24	28	28	25	25	0.58	0.58
25	24	29	29	32	32	0.96	0.96
35	34	29	29	32	32	1.01	1.01
48	48	32	32	40	40	1.45	1.45
50	50	32	32	40	40	1.47	1.47
50	51	32.5	32.5	40	40	1.65	1.65
55	50	33	33	40	40	1.69	1.69
59	60	33	33	50	50	1.84	1.84
60	59	33	33	63	63	2.59	2.59
68	65	34	34	80	80	2.75	2.75

Table 4.8 shows that the kVp and mAs were increased when increasing CBT. Similarly, the MGD was therefore increased. For patients of age range [40 – 49 years] the mean MGD was 1.59 mGy and range (from 0.58 mGy to 2.75 mGy) for both RCC and LCC projection views.

Table 4.9 below, shows how the technique factors selected by operators (manual mode) and the mean glandular dose per views vary when the breast thickness varies for patient within age range of [50 - 64].

Table 4.9: Variation of MGD, kVp, mAs against CBT for patients age [50 - 64]

Age Range [50 – 64]							
CBT (mm)		**kVp (kV)**		**mAs (mAs)**		**MGD (mGy)**	
RCC	**LCC**	**RCC**	**LCC**	**RCC**	**LCC**	**RCC**	**LCC**
20	18.7	30	30	30	30	1.10	1.10
35	36	31	31	32	32	1.16	1.16
45	45	32	32	40	40	1.41	1.41
45	44	32	32	40	40	1.96	1.96
48	47	32	32	40	40	1.98	1.98
49	48	32.5	32.5	50	50	2.06	2.06
51	50	33	32	50	50	2.12	2.12
51	50.6	33	33	50	50	2.12	2.12
55	54	33	33	50	50	2.16	2.16
60	62	35	35	50	50	2.18	1.90
65	65	35	35	50	50	2.18	2.18

It can be deduced from the table 4.9 analysis that kVp and mAs were increased following the increase in the CBTs. Similarly, MGD was increased for patients of age range [50 – 64 years]. The mean MGD was 1.86 mGy, range (from 1.10 mGy to 2.18 mGy) for RCC projection views and was 1.83 mGy, range (from 1.10 mGy to 2.18 mGy) for LCC projection views.

Table 4.10, presents the comparison of the calculated MGD for patients with age within [40 – 49 years] to IAEA Human Health Series (IAEA HHS) No.17 standards values established according to specific equivalent compressed breast thickness (Eq CBT).

Table 4.10: Comparison of patients MGD to IAEA Standards, age range of [40 - 49]

Age Range [40 - 49]

Eq CBT (mm)	CBT (mm)		MGD (mGy)		Ext Std MGD (mGy)		IAEA Standards MGD (mGy)
	RCC	LCC	RCC	LCC	RCC	LCC	
21							<1
	25	24	0.58	0.58	1	0.9	
	25	24	0.96	0.96	1	0.9	
32							<1.5
	35	34	1.01	1.01	1.6	1.6	
45							<2
	48	48	1.45	1.45	2.4	2.4	
	50	50	1.47	1.47	2.6	2.6	
	50	51	1.65	1.65	2.6	2.6	
53							<2.5
	55	50	1.69	1.69	2.9	2.6	
	59	60	1.84	1.84	3.1	3	
60	60	59	2.59	2.59	3	3.1	<3
	68	65	2.75	2.75	3.7	3.5	
75							<4.5

For the actual patient age range, the CBTs varied from 24 mm to 68 mm. For more accurate comparison, the IAEA Standards values were extrapolated according to each patient CBT. This allows obtaining the extrapolated standards MGD (Ext Std MGD) values corresponding to each patient CBT recorded. Then the estimated MGD values were compared to the Ext Std MGD values. It can be derived from analysis of table 4.10 that all patients with CBT from 24 mm to 68 mm have received less dose either for RCC views or for LCC views. This results demonstrate was that there was

no over exposure from the mammography unit at CHUD/OP for patients within the age range of [40 – 49 years].

Table 4.1 presents the comparison of the calculated MGD for patients with age within [50 – 64 years] to IAEA Human Health Series (IAEA HHS) No.17 standards values established according to specific equivalent compressed breast thickness (Eq CBT).

Table 4.11: Comparison of patients MGD to IAEA Standards, age range [50 – 64 years]

Age Range [50 - 64]

Eq CBT (mm)	CBT (mm)		MGD (mGy)		Ext Std MGD		IAEA Standards (mGy)
	RCC	LCC	RCC	LCC	RCC	LCC	
	20	18.7	1.10	1.10	0.7	0.6	
21							<1
32							<1.5
	35	36	1.16	1.16	1.6	1.7	
45	45	45	1.41	1.41	2	2	<2
	45	44	1.96	1.96	2	2.2	
	48	47	1.98	1.98	2.4	2.4	
	49	48	2.06	2.06	2.5	2.4	
	51	50	2.12	2.12	2.6	2.6	
	51	50.6	2.12	2.12	2.9	2.6	
53							<2.5
	55	54	2.16	2.16	3	2.8	
60	60	62	2.18	1.90	3.5	3	<3
	65	65	2.18	2.18		3.5	
75							<4.5

For patients within the age range of [50 – 64 years] the CBT varied from 18.7 mm to 65 mm. So for more accurate comparison, the IAEA standards values were used to obtain the extrapolated standards MGD (Ext Std MGD) values corresponding to each

patient CBT recorded. These values were then used to make the comparison. It could be derived from analysis of Table 4.10 that all patients having CBT from 35 mm to 65 mm received less dose either for RCC views or for LCC views. Except the patient having a CBT of 20 mm for RCC and 18.7 mm for LCC received a slightly high dose (1.10 mGy for both breast) than the standards limits (1 mGy at 21 mm CBT).

The results demonstrate that there was no over exposure from the mammography unit at CHUD/OP for patients within the age range of [50 – 64 years] when the breast thicknesses were within the range of equivalent compressed breast thickness. But when the CBT was less than the minimum equivalent breast thickness an overexposure could occur.

CHAPTER FIVE

CONCLUSION AND RECOMANDATIONS

5.1 Conclusion

The quality control assessment was performed on the three mammography machines selected for this study following the IAEA Human Health Series No.2 and No.17 protocols. The assessment done included kVp accuracy and repeatability, output repeatability and linearity, Half Value Layer measurement, image quality test based on subjective analysis and compression test. The results obtained confirmed that all the machines are working correctly and were within acceptable performance criteria. The MGD was estimated using manual exposure mode as well as the AEC mode. The MGDs obtained under the two exposure modes were compared with the IAEA Human Health Series No.17. It was found that less radiation dose was delivered under the AEC mode. The dose difference between AEC mode and manual mode was 1.31 mGy for CHUD/OP and 1.01 mGy for CAR respectively.

The radiation dose delivered to patients undergoing diagnostic as well as screening mammography examination at CHUD/OP was also estimated. The MGD per RCC view and LCC view was estimated for each patient classified in two age ranges [40 – 49 years] and [50 – 64 years]. It is confirmed, based on the calculated MGD from patient with various compressed breast thicknesses, that there was no overexposure during mammography examination for patients aged [40 – 49 years] and [50 – 64 years]. However, a higher dose (1.10 mGy for RCC and LCC) was calculated for patient breast thickness less than 20 mm within age range of [50 – 64 years].

5.2 Recommendations

Based on the results and the conclusion of this research, the following recommendations are addressed to relevant stakeholders to achieve optimization of patient radiation protection in mammography practices.

5.2.1 Government authorities

Since the Nuclear Law is promulgated, it is very important that the Atomic Energy Commission and the Regulatory Authority be created in aim to regulate the use of ionizing radiation in Benin.

5.2.2 Health Ministry

A National Quality Assurance programme for the use of ionizing radiation sources, adapted to local conditions should be developed and implemented. This will help to improve mammography practice in term of optimization in Benin.

5.2.3 Hospital authorities

The employment of Medical Physicist is recommended for them to undertake quality control on medical equipment. Optimum equipment leads to optimization of practices.

5.2.3 Radiographers

Since the exposure parameters are radiographers choice based, patient dose optimization should be a priority in all facilities to minimise radiation-induced cancer from over exposure. The best way would be to use the AEC mode during patient examinations.

REFERENCES

(IARC), I. A. for R. on C. (2015). Fact Sheets by Cancer. Retrieved April 10, 2018, from http://globocan.iarc.fr/Pages/fact_sheets_cancer.aspx

Aggarwal, latit M. (2016). Biological Effects of Ionizing Radiation . Biological Effects of Ionizing Radiation, (January 2014).

Akrobortu, E., Boadu, M., Yeboah, J., Schandoff, C., & Gyekye, P. K. (2013). Inter-Comparison of Dose Indicators and Mean Glandular Dose for some Selected Diagnostic Mammography Units in Accra , Ghana, *3*(5), 291–295.

Assiamah, M., Nam, T. L., & Keddy, R. J. (2005). Comparison of mammography radiation dose values obtained from direct incident air kerma measurements with values from measured X-ray spectral data. *Applied Radiation and Isotopes*, *62*(4), 551–560. https://doi.org/10.1016/j.apradiso.2004.09.010

Camargo-Mendoza, R. E., Poletti, M. E., Costa, A. M., & Caldas, L. V. E. (2011). Measurement of some dosimetric parameters for two mammography systems using thermoluminescent dosimetry. *Radiation Measurements*, *46*(12), 2086–2089. https://doi.org/10.1016/j.radmeas.2011.06.019

Committee, C. S. (2004a). ACR PRACTICE GUIDELINE FOR THE PERFORMANCE OF SCREENING MAMMOGRAPHY, 245–256.

Committee, C. S. (2004b). ACR Practice Guideline for the Performance of Scrotal, 545–547.

Committee, C. S. (2006). ACR Practice Guideline for the Performance of Screening Mammography, 467–478.

D. Dance, S. Christofides, M. Maidment, I. M. (2014). Diagnostic Radiology Physics: A handbook for teachers and students. *Iaea*, 710. Retrieved from http://www-pub.iaea.org/books/IAEABooks/8841/Diagnostic-Radiology-Physics-A-Handbook-for-Teachers-and-Students?utm_content=buffer89b0e&utm_medium=social&utm_source=twitter.com&utm_campaign=buffer

Dance, D. R., Skinner, C. L., Young, K. C., Beckett, J. R., & Kotre, C. J. (2000). Additional factors for the estimation of mean glandular breast dose using the UK mammography dosimetry protocol. *Physics in Medicine and Biology*, *45*(11), 3225–3240. https://doi.org/10.1088/0031-9155/45/11/308

DAVISSON, C. M. (1968). Interaction of Radiation with Matter. *Alpha-, Beta- and Gamma-Ray Spectroscopy*, 37–78. https://doi.org/http://dx.doi.org/10.1016/B978-0-7204-0083-0.50007-9

de Rinaldis, E., Tutt, A., & Dontu, G. (2011a). Breast Cancer. In *Breast Pathology* (pp. 352–359). https://doi.org/10.1016/B978-1-4377-1757-0.00028-7

de Rinaldis, E., Tutt, A., & Dontu, G. (2011b). Breast Cancer. In *Breast Pathology* (pp. 352–359). https://doi.org/10.1016/B978-1-4377-1757-0.00028-7

EFOMP Protocol, M. (2015). E F O M P, (March).

Ferlay, J., Soerjomataram, I., Dikshit, R., Eser, S., Mathers, C., Rebelo, M., … Bray, F. (2015). Cancer incidence and mortality worldwide: Sources, methods and major patterns in GLOBOCAN 2012. *International Journal of Cancer*, *136*(5), E359–E386. https://doi.org/10.1002/ijc.29210

Hendrick, R. E. (2010). Radiation Doses and Cancer Risks from Breast Imaging Studies. *Radiology*, *257*(1), 246–253. https://doi.org/10.1148/radiol.10100570

Http://www.imaginis.com/breast-health-101-cancer/breast-anatomy-and-physiology 2/1997. (n.d.). Breast Anatomy and Physiology | Breast Health 101 | Imaginis - The Women's Health & Wellness Resource Network. Retrieved July 14, 2018, from http://www.imaginis.com/breast-health-101-cancer/breast-anatomy-and-physiology-2

Https://clinicalgate.com. (n.d.). Mammography Acquisition: Screen-Film and Digital Mammography, the Mammography Quality Standards Act, and Computer-Aided Detection | Clinical Gate. Retrieved June 2, 2018, from https://clinicalgate.com/mammography-acquisition-screen-film-and-digital-mammography-the-mammography-quality-standards-act-and-computer-aided-detection/

Https://www.webmd.com/women/picture-of-the-breasts#1/2014. (n.d.). The Breast (Human Anatomy): Picture, Function, Conditions, & More. Retrieved July 14, 2018, from https://www.webmd.com/women/picture-of-the-breasts#1

IAEA. (2014). Dosimetry in Diagnostic Radiology: an Internacional Code of Practice. *Igarss 2014*, (1), 1–5. https://doi.org/10.1007/s13398-014-0173-7.2

International Atomic Energy Agency. (2009). IAEA HumAN HEAltH SErIES Screen Film Mammography, (2). Retrieved from http://www-pub.iaea.org/MTCD/publications/PDF/Pub1381_web.pdf

Marianne, C., & Bengt, A. (2008). Absorbed Dose Measurement in Mammography.

Miglioretti, D. L., Lange, J., Van Den Broek, J. J., Lee, C. I., Van Ravesteyn, N. T., Ritley, D., … Hubbard, R. A. (2016). Radiation-induced breast cancer incidence and mortality from digital mammography screening a modeling study. *Annals of Internal Medicine*, *164*(4), 205–214. https://doi.org/10.7326/M15-1241

Monticciolo, D. L., Newell, M. S., Hendrick, R. E., Helvie, M. A., Moy, L., Monsees, B., … Sickles, E. A. (2017). Breast Cancer Screening for Average-Risk Women: Recommendations From the ACR Commission on Breast Imaging. *Journal of the American College of Radiology*, *14*(9), 1137–1143. https://doi.org/10.1016/j.jacr.2017.06.001

Nikjoo, H., Uehara, S., & Emfietzoglou, D. (2012). *Interaction of radiation with matter*. Retrieved from http://www.sprawls.org/ppmi2/INTERACT/#Photon Interactions

Phantom Mammo ACR Gammex 156 SimpliBuy. (n.d.). Retrieved July 20, 2018, from http://www.simplibuy.ca/product/details/10791

Reis, C., Pascoal, A., Sakellaris, T., & Koutalonis, M. (2013). Quality assurance and quality control in mammography: A review of available guidance worldwide. *Insights into Imaging*, *4*(5), 539–553. https://doi.org/10.1007/s13244-013-0269-1

Shah, D. J., Sachs, R. K., & Wilson, D. J. (2012). Radiation-induced cancer: a modern view. *The British Journal of Radiology*, *85*(1020), e1166-73. https://doi.org/10.1259/bjr/25026140

Ślusarczyk-Kacprzyk, W., Skrzyński, W., & Fabiszewska, E. (2016). Evaluation of Doses and Image Quality in Mammography with Screen-Film, CR, and DR Detectors – Application of the ACR Phantom. *Polish Journal of Radiology*, *81*, 386–391. https://doi.org/10.12659/PJR.897304

Sosu, E. K., Boadu, M., & Mensah, S. Y. (2018). Determination of dose delivery accuracy and image quality in full - Field digital mammography. *Journal of Radiation Research and Applied Sciences*. https://doi.org/10.1016/j.jrras.2018.02.002

Sprawls, P. (2015). The physics and technology of mammography - for effective clinical imaging. Retrieved July 15, 2018, from http://www.sprawls.org/resources/MAMMO/module.htm#13/

Www.ncbi.nlm.nih.gov/books/NBK65716/figure/CDR0000062970__281/. (2018). https://www.ncbi.nlm.nih.gov/books/NBK65716/figure/CDR0000062970__281/. Retrieved July 16, 2018, from https://www.ncbi.nlm.nih.gov/books/NBK65716/figure/CDR0000062970__281

APENDICES

APPENDIX A: DATA COLLECTION

Appendix A1: Data sheet of equipment information

	CHARACTERISTIQUES	OBSERVATIONS	
1	Type of equipment	Screen-Film	CR
2	Manufacturer		
3	Model		
4	Year of make		
5	Serial number		
6	Mode of operation		
7	Anode/filter material		
8	Filtration		
9	kVp range	Min	Max
10	mAs range	Min	Max

Appendix A2: Data sheet for Patients information

N°	PARAMETERS	OBSERVATIONS			Height	Weight
1	**Identification**					
2	**Age of patient**					
3	**Type of radiography**	**Diagnostic**			**Screening**	
4	**Breast number imaged**	**Right**			**Left**	
5	**Breast view taken**	**RCC**	**RML**	**ROBL**	**LCC**	**LML**	**LOBL**
6	**CBT(mm)**						
7	**kVp**						
8	**mAs**						
9	**ESAK**						
10	**MGD(mGy)**						

Appendix A3: Mammography unit assembly assessment

PARAMETER	FACILITIES		
	SAA	CAR	CHUD/OP
Mechanical stability of free-standing unit			
Lights indicator			
Units motion function			
Locks and detents function			
Angulation indicators			
Wobble and vibration Image receptors sliding and holding during gantry angulation			
Compression paddle condition			
Automatic compression release			
Operator shielding evaluation			
Safety of patient/operator against units			
Availability of technique parameters chart			

APPENDIX B: QUALITY CONTROL TESTS

Appendix B1: kVp Accuracy and repeatability test

Table for kvp accuracy and repeatability	
kVp_{nom}	
mAs	
Measured kVp values	
kVp_{mea1}	
kVp_{mea2}	
Repeatability : Difference (%)	
Additional measured kVp	
kVp_{mea3}	
kVp_{mea4}	
kVp_{mea5}	
Average of kVp_{mea}	
SD (%)	
Repeatability : Coefficient of Variance(%)	
Accuracy Deviation (%)	
Tolerance	
REPEATABILITY COV(%)	
Accuracy DEV (%)	

Appendix B2: Output repeatability and linearity

Distance focus-dosimeter (mm)			
kVp_{nom} set			
mAs_1 set	**40**	**$ESAK_{mea1}$**	
		$ESAK_{mea2}$	
		$ESAK_{mea3}$	
		$ESAK_{mea4}$	
		$ESAK_{mea5}$	
Repeatability Coefficient of Variation (%) ≤ 5%		**Average of $ESAK_{mea}$**	
		Standard Deviation	
		COV(%)	
		Output (y_1)	
mAs_2 set	**80**	**$ESAK_{mea1}$**	
		$ESAK_{mea2}$	
		Average of $ESAK_{mea}$	
		Output (y_2)	
mAs_3 set	**125**	**$ESAK_{mea1}$**	
		$ESAK_{mea2}$	
		Average of $ESAK_{mea}$	
		Output (y_3)	
Linearity		**L_1**	
		L_2	
Average output			
Normalyzed output (mGy/mAs at 1m			

Tolerance	
Repeatability	
Linearity	
Normalyzed Output(µGy at 1m) should be > 30µGy/mAs	

Appendix B3: Data sheet for HVL measurement

Half Value Layer CAR					Tolerance
kVp_{set}	**kV_{mea}**	**HVL_{mea} (mm Al)**	**(kVp/100)+0,03**	**(kVp/100)+c**	**HVL**

Appendix B4: Data sheet for AEC repeatability

Tk_{PMMA}	**kVp_{mea} (kV)**	**mAs_{dis} $(mAs)_{mea}$**	**SD**	**MEAN**	**Coefficient of variance**

Appendix B5: Data sheet for Compression tests

Compression Tests	**RF(cm)**	**LF(cm)**	**Difference (%)**	**Interpretation**
Alignment				
Thickness	**Tk_{set}**	**Tk_{mea}**	**DEV(%)**	**Interpretation**
Force	**Measurement (kG)**	**Force (N)**		**Interpretation**
Manual				
Automatic				

APPENDIX C: TABULATED CONVERSION FACTORS USED MGD CALCULATION

Appendix C1: g-factors (mGy/mGy) for breast thickness of 2-11 cm and the HVL range 0.30-0.60 mm Al.

Breast thickness (cm)	HVL (mm Al)						
	0.30	0.35	0.40	0.45	0.50	0.55	0.60
2	0.390	0.433	0.473	0.509	0.543	0.573	0.587
3	0.274	0.309	0.342	0.374	0.406	0.437	0.466
4	0.207	0.235	0.261	0.289	0.318	0.346	0.374
4.5	0.183	0.208	0.232	0.258	0.285	0.311	0.339
5	0.164	0.187	0.209	0.232	0.258	0.287	0.310
6	0.135	0.154	0.172	0.192	0.214	0.236	0.261
7	0.114	0.130	0.145	0.163	0.177	0.202	0.224
8	0.098	0.112	0.126	0.140	0.154	0.175	0.195
9	0.0859	0.0981	0.1106	0.1233	0.1357	0.1543	0.1723
10	0.0763	0.0873	0.0986	0.1096	0.1207	0.1375	0.1540
11	0.0687	0.0786	0.0887	0.0988	0.1088	0.1240	0.1385

IAEA (2000, 2009)

Appendix C2: s-factors for clinically used spectra and maximum errors that can be incurred when they are used.

Spectrum	*s*-factor	Maximum error (%)
Mo/Mo	1.000	3.1
Mo/Rh	1.017	2.2
Rh/Rh	1.061	3.6
Rh/Al	1.044	2.4
W/Rh	1.042	2.1

IAEA (2000, 2009)

Appendix C3: c-factors for glandularity of 0.1-100% in the central region of the breast, breast thickness of 2-11 cm and HVL of 0.30-0.60 mm Al

HVL (mm Al)	Thickness (cm)	Breast glandularity				
		0.1%	25%	50%	75%	100%
0.30	2	1.130	1.059	1.000	0.938	0.885
0.30	3	1.206	1.098	1.000	0.915	0.836
0.30	4	1.253	1.120	1.000	0.898	0.808
0.30	5	1.282	1.127	1.000	0.886	0.794
0.30	6	1.303	1.135	1.000	0.882	0.785
0.30	7	1.317	1.142	1.000	0.881	0.784
0.30	8	1.325	1.143	1.000	0.879	0.780
0.30	9	1.328	1.145	1.000	0.879	0.780
0.30	10	1.329	1.147	1.000	0.880	0.780
0.30	11	1.328	1.143	1.000	0.879	0.779
0.35	2	1.123	1.058	1.000	0.943	0.891
0.35	3	1.196	1.090	1.000	0.919	0.842
0.35	4	1.244	1.112	1.000	0.903	0.816
0.35	5	1.272	1.121	1.000	0.890	0.801
0.35	6	1.294	1.132	1.000	0.886	0.793
0.35	7	1.308	1.138	1.000	0.886	0.788
0.35	8	1.312	1.140	1.000	0.884	0.786
0.35	9	1.319	1.145	1.000	0.884	0.786
0.35	10	1.319	1.144	1.000	0.881	0.785
0.35	11	1.322	1.142	1.000	0.882	0.784
0.40	2	1.111	1.054	1.000	0.949	0.900
0.40	3	1.181	1.087	1.000	0.922	0.851
0.40	4	1.227	1.105	1.000	0.907	0.825
0.40	5	1.258	1.120	1.000	0.899	0.810
0.40	6	1.276	1.125	1.000	0.890	0.798
0.40	7	1.292	1.132	1.000	0.887	0.793
0.40	8	1.302	1.136	1.000	0.885	0.790
0.40	9	1.308	1.138	1.000	0.884	0.789
0.40	10	1.311	1.138	1.000	0.883	0.788
0.40	11	1.315	1.140	1.000	0.885	0.791
0.45	2	1.099	1.052	1.000	0.948	0.905
0.45	3	1.169	1.080	1.000	0.924	0.858
0.45	4	1.209	1.102	1.000	0.909	0.829
0.45	5	1.248	1.115	1.000	0.898	0.815
0.45	6	1.267	1.125	1.000	0.891	0.801
0.45	7	1.283	1.129	1.000	0.892	0.797
0.45	8	1.298	1.137	1.000	0.887	0.799
0.45	9	1.301	1.135	1.000	0.886	0.792
0.45	10	1.305	1.138	1.000	0.886	0.791
0.45	11	1.312	1.138	1.000	0.885	0.789
0.50	2	1.098	1.050	1.000	0.955	0.910
0.50	3	1.164	1.078	1.000	0.928	0.864
0.50	4	1.209	1.094	1.000	0.912	0.835
0.50	5	1.242	1.111	1.000	0.903	0.817
0.50	6	1.263	1.120	1.000	0.896	0.807
0.50	7	1.278	1.127	1.000	0.890	0.800
0.50	8	1.289	1.132	1.000	0.889	0.794
0.50	9	1.295	1.134	1.000	0.887	0.793
0.50	10	1.302	1.138	1.000	0.886	0.791
0.50	11	1.303	1.140	1.000	0.885	0.789

Appendix C3 (continued)

HVL (mm Al)	Thickness (cm)	Breast glandularity				
		0.1%	25%	50%	75%	100%
0.55	2	1.086	1.043	1.000	0.955	0.914
0.55	3	1.154	1.071	1.000	0.932	0.870
0.55	4	1.196	1.093	1.000	0.918	0.843
0.55	5	1.227	1.105	1.000	0.906	0.824
0.55	6	1.252	1.115	1.000	0.900	0.814
0.55	7	1.267	1.122	1.000	0.896	0.805
0.55	8	1.278	1.125	1.000	0.890	0.800
0.55	9	1.285	1.128	1.000	0.890	0.798
0.55	10	1.290	1.133	1.000	0.889	0.796
0.55	11	1.293	1.134	1.000	0.888	0.793
0.60	2	1.089	1.045	1.000	0.959	0.919
0.60	3	1.142	1.065	1.000	0.933	0.874
0.60	4	1.185	1.090	1.000	0.923	0.850
0.60	5	1.216	1.102	1.000	0.910	0.830
0.60	6	1.238	1.113	1.000	0.904	0.820
0.60	7	1.252	1.120	1.000	0.899	0.812
0.60	8	1.266	1.123	1.000	0.894	0.806
0.60	9	1.272	1.124	1.000	0.893	0.801
0.60	10	1.279	1.125	1.000	0.891	0.797
0.60	11	1.284	1.129	1.000	0.893	0.798

Appendix C4: c-factors for average breast for women in age group 40 to 49

Breast thickness (cm)	HVL (mm Al)						
	0.30	0.35	0.40	0.45	0.50	0.55	0.60
2	0.885	0.891	0.900	0.905	0.910	0.914	0.919
3	0.894	0.898	0.903	0.906	0.911	0.915	0.918
4	0.940	0.943	0.945	0.947	0.948	0.952	0.955
5	1.005	1.005	1.005	1.004	1.004	1.004	1.004
6	1.080	1.078	1.074	1.074	1.071	1.068	1.066
7	1.152	1.147	1.141	1.138	1.135	1.130	1.127
8	1.220	1.213	1.206	1.205	1.199	1.190	1.183
9	1.270	1.264	1.254	1.248	1.244	1.235	1.225
10	1.295	1.287	1.279	1.275	1.272	1.262	1.251
11	1.294	1.290	1.283	1.281	1.273	1.264	1.256

Appendix C5: c-factors for average breast for women in age group 50 to 64

Breast thickness (cm)	HVL (mm Al)						
	0.30	0.35	0.40	0.45	0.50	0.55	0.60
2	0.885	0.891	0.900	0.905	0.910	0.914	0.919
3	0.925	0.929	0.931	0.933	0.937	0.940	0.941
4	1.000	1.000	1.000	1.000	1.000	1.000	1.000
5	1.086	1.082	1.081	1.078	1.075	1.071	1.069
6	1.164	1.160	1.151	1.150	1.144	1.139	1.134
7	1.232	1.225	1.214	1.208	1.204	1.196	1.188
8	1.275	1.265	1.257	1.254	1.247	1.237	1.227
9	1.299	1.292	1.282	1.275	1.270	1.260	1.249
10	1.307	1.298	1.290	1.286	1.283	1.272	1.261
11	1.306	1.301	1.294	1.291	1.283	1.274	1.266

Appendix C6: Acceptable and achievable limits for Mean Glandular Dose (D_G)

TABLE 21. ACCEPTABLE AND ACHIEVABLE LIMITS FOR MEAN GLANDULAR DOSE (D_G)

Thickness of PMMA (mm)	Thickness of equivalent breast (mm)	Acceptable level for D_G to equivalent breast (mGy)	Achievable level for D_G to equivalent breast (mGy)
20	21	1.0	0.6
30	32	1.5	1.0
40	45	2.0	1.6
45	53	2.5	2.0
50	60	3.0	2.4
60	75	4.5	3.6
70	90	6.5	5.1

APPENDIX D: TABLES OF CALCULATED OUTPUT, ESAK, MGD AND CONVERSION FACTEORS FOR EACH FACILITY

Appendix D1: Calculated MGD at SAA

CBT (mm)	kVp_{set} (kV)	kVp_{mea} (kV)	$ESAK_i$ (mGy)	HVL (mm Al)	mAs_{set}	ESAK (mGy)	D_1 (mm)	D_2 (mm)	g	c	s	MGD (mGy)	Output (mGy/mAs)
30	25	24,969	3,179	0,31	32	3,528	590	560	0,28178	1	1	0,994	0,099
40	26	26,058	3,610	0,32	32	4,154	590	550	0,2182	1	1	0,906	0,113
45	27	27,104	4,604	0,33	36	5,396	590	545	0,198	1	1	1,068	0,128
50	28	28,295	5,705	0,34	40	6,810	590	540	0,1824	1	1	1,242	0,143
60	28	28,188	6,429	0,34	45	7,967	590	530	0,1502	1	1	1,197	0,143
70	28	28,250	7,130	0,34	50	9,179	590	520	0,1268	1	1	1,164	0,143

Appendix D2: Calculated MGD from CAR using the manual mode

CBT (mm)	kVp_{set} (kV)	kV_{mea} (kV)	$ESAK_i$ (mGy)	HVL (mm Al)	mAs_{set}	ESAK	D_1 (mm)	D_2 (mm)	g	c	s	MGD (mGy)	Output (mGy/mAs)	Average MGD (mGy)
30	25	25,103	2,891	0,32	45	3,183	640	610	0,288	1	1	0,917	0,064	
40	28	27,923	4,637	0,35	50	5,275	640	600	0,235	1	1	1,240	0,093	
45	29	28,920	5,763	0,35	56	6,668	640	595	0,208	1	1	1,387	0,103	
50	29	28,937	5,768	0,35	56	6,787	640	590	0,187	1	1	1,269	0,103	1,3
60	30	30,038	8,061	0,36	71	9,816	640	580	0,158	1	1	1,547	0,114	
70	30	30,005	10,225	0,36	90	12,891	640	570	0,133	1	1	1,714	0,114	

Appendix D3: Calculated MGD from CAR using the AEC mode

CBT (mm)	kVp_{mea} (kV)	$ESAK_i$ (mGy)	HVL (mm Al)	mAs	$ESAK_{AEC}$ (mGy)	D_1 (mm)	D_2 (mm)	g	c	s	MGD (mGy)	Output (mGy/mAs)	Average MGD (mGy)
30	26,037	3,229	0,33	12,3	3,555	640	610	0,295	1	1	1,049	0,263	
40	26,033	3,235	0,33	13,2	3,680	640	600	0,224	1	1	0,824	0,245	
45	26,086	3,230	0,33	12,7	3,737	640	595	0,198	1	1	0,740	0,254	0,674
50	26,044	3,243	0,33	12,9	3,816	640	590	0,165	1	1	0,517	0,251	
60	26,089	3,226	0,33	12,7	3,928	640	580	0,136	1	1	0,450	0,254	
70	26,105	3,233	0,33	13,1	4,076	640	570	0,114	1	1	0,467	0,247	

Appendix D4: Calculated MGD from CHUD/OP using the manual mode

CBT (mm)	kVp_{set} (kV)	kV_{mea} (kV)	$ESAK_i$ (mGy)	HVL (mm Al)	mAs_{set}	ESAK (mGy)	D_1 (mm)	D_2 (mm)	g	c	s	MGD (mGy)	Output (mGy/mAs)	Average MGD (mGy)
30	31	33,170	5,488	0,38	40	6,091	590	560	0,3318	1	1	2,021	0,137	
40	31,5	33,814	7,220	0,38	50	8,309	590	550	0,2506	1	1	2,082	0,144	
45	32	34,264	9,216	0,39	50	10,801	590	545	0,2272	1	1	2,454	0,184	1,637
50	32	34,266	7,367	0,39	50	8,795	590	540	0,2046	1	1	1,799	0,147	
60	32	34,188	7,382	0,38	63	9,148	590	530	0,1648	1	1	1,508	0,117	
70	33	35,439	10,078	0,39	63	12,974	590	520	0,142	1	1	1,842	0,160	

Appendix D5: Calculated MGD from CHUD/OP using the AEC mode

CBT (mm)	kVp_{set} (kV)	kV_{mea} (kV)	$ESAK_i$ (mGy)	HVL (mm Al)	mAs_{mea}	$ESAK_{AEC}$ (mGy)	D_1 (mm)	D_2 (mm)	g	c	s	MGD (mGy)	Output (mGy/mAs)	Average MGD (mGy)
30	25,5	27,309	1,384	0,33	12,3	1,536	590	560	0,295	1	1	0,453	0,112	
40	25,5	27,421	1,351	0,33	12,5	1,554	590	550	0,2238	1	1	0,348	0,108	
45	25,5	27,443	1,302	0,33	12,7	1,526	590	545	0,198	1	1	0,302	0,103	0,305
50	25,5	27,380	1,324	0,33	12,9	1,580	590	540	0,1778	1	1	0,281	0,103	
60	25,5	27,360	1,306	0,33	12,7	1,618	590	530	0,1464	1	1	0,237	0,103	
70	25,5	27,432	1,329	0,33	13,2	1,710	590	520	0,1236	1	1	0,211	0,101	

Appendix D6: Calculated MGD of patients from CHUD/OP

N° of patient	Age	kVp (kV)		mAs (mAs)		CBT (mm)		Output (mGy/mAs)		$ESAK_i$ (mGy)			Conversion factor			MGD (mGy)	
		RCC	LCC	RCC	LCC	RCC	LCC	RCC	LCC	RCC	LCC	HVL	g	c	s	RCC	LCC
1	63	32	32	50	50	51	50,6	0,18	0,18	8,95	8,95	0,38	0,2046	1,081	1	1,98	1,98
2	40	29	29	32	32	35	34	0,10	0,10	3,18	3,18	0,38	0,3251	0,925	1	0,96	0,96
3	54	32	32	50	50	45	45	0,18	0,18	8,95	8,95	0,38	0,2272	1,041	1	2,12	2,12
4	50	32,5	32,5	50	50	51	50	0,19	0,19	9,61	9,61	0,38	0,2045	1,081	1	2,12	2,12
5	41	28	28	25	25	25	24	0,07	0,07	1,83	1,83	0,38	0,3531	0,9	1	0,58	0,58
6	53	33	32	30	30	20	18,7	0,21	0,18	6,17	5,37	0,38	0,3531	1,001	1	2,18	1,90
7	45	32	32	50	50	55	50	0,18	0,18	8,95	8,95	0,38	0,2045	1,005	1	1,84	1,84
8	42	29	29	32	32	25	24	0,10	0,10	3,18	3,18	0,38	0,3531	0,9	1	1,01	1,01
9	63	31	31	40	40	48	47	0,15	0,15	6,10	6,10	0,38	0,1998	0,9	1	1,10	1,10
10	46	33	33	80	80	68	65	0,21	0,21	16,44	16,44	0,39	0,152	1,1	1	2,75	2,75
11	42	34	34	63	63	60	59	0,23	0,23	14,62	14,62	0,39	0,1648	1,074	1	2,59	2,59
12	51	32	32	50	50	49	48	0,18	0,18	8,95	8,95	0,39	0,2175	1,005	1	1,96	1,96
13	40	32	32	40	40	50	50	0,18	0,18	7,16	7,16	0,39	0,2046	1,005	1	1,47	1,47
14	61	30	30	40	40	45	44	0,13	0,13	5,04	5,04	0,39	0,2272	1,0115	1	1,16	1,16
15	40	32,5	32,5	40	40	48	48	0,19	0,19	7,69	7,69	0,39	0,2136	1,002	1	1,65	1,65
16	44	33	33	40	40	59	60	0,21	0,21	8,22	8,22	0,39	0,1648	1,074	1	1,45	1,45
17	54	33	33	32	32	35	36	0,21	0,21	6,58	6,58	0,39	0,2851	1,151	1	2,16	2,16
18	43	33	33	40	40	50	51	0,21	0,21	8,22	8,22	0,39	0,2046	1,005	1	1,69	1,69
19	64	35	35	50	50	60	62	0,26	0,26	12,93	12,93	0,39	0,1648	1,025	1	2,18	2,18
20	63	33	33	50	50	65	65	0,21	0,21	10,28	10,28	0,39	0,1448	0,951	1	1,41	1,41
21	58	35	35	40	40	55	54	0,26	0,26	10,34	10,34	0,39	0,1984	1,002	1	2,06	2,06

APPENDIX E: RAW DATA COLLECTED

Appendix E1: Raw Data from SAA

	Set kV (kVnom)	Tube voltage (kVmea)	Exposure time (ms)	Exposure (mGy)	Exposure rate (mGy/s)	HVL (mm Al)
kVp accuracy and repeatability						
	28	28,149	402,483	5,516	13,569	0,342
	28	28,110	402,473	5,521	13,547	0,342
	28	28,086	402,998	5,522	13,583	0,342
	28	28,113	402,482	5,525	13,573	0,342
	28	28,157	402,473	5,515	13,566	0,342
Half Value Layer	**Set kV (kVnom)**	**Tube voltage (kVmea)**	**Exposure time (ms)**	**Exposure (mGy)**	**Exposure rate (mGy/s)**	**HVL (mm Al)**
	22	21,659	264,492	1,514	5,661	0,257
	25	24,938	324,710	3,066	9,328	0,307
	28	28,086	402,998	5,522	13,583	0,342
	31	31,504	580,656	10,461	17,906	0,370
Output repeatability and linearity						
Output@ 40mAs	**Set kV (kVnom)**	**Tube voltage (kVmea)**	**Exposure time (ms)**	**Exposure (mGy)**	**Exposure rate (mGy/s)**	**HVL (mm Al)**
	28	28,149	402,483	5,516	13,569	0,342
	28	28,110	402,473	5,521	13,547	0,342
Output @ 80mAs						
	28	28,120	802,484	11,042	13,682	0,342
	28	28,084	802,465	11,049	13,691	0,342
Output @ 125mAs						
	28	28,110	1251,136	17,253	13,745	0,342
	28	28,121	1251,131	17,255	13,747	0,342

Appendix E2: Raw Data from SAA (continued)

MGD (mm)	Set kV (kV_{nom})	Tube voltage (kV_{mea})	Exposure time (ms)	Exposure (mGy)	Exposure rate (mGy/s)	HVL (mm Al)
30	25	24,969	324,700	3,179	9,699	0,308
30	25	24,979	502,347	4,957	9,789	0,308
40	26	26,058	324,165	3,610	10,997	0,321
40	26	26,072	501,869	5,627	11,133	0,320
45	27	27,104	362,831	4,604	12,567	0,332
45	27	27,130	501,343	6,381	12,626	0,332
50	28	28,295	402,473	5,705	13,981	0,343
50	28	28,253	501,840	7,131	14,109	0,343
60	28	28,188	452,162	6,429	14,108	0,343
60	28	28,240	501,840	7,135	14,118	0,343
70	28	28,250	501,371	7,130	14,093	0,343

Appendix E3: Raw Data from CAR

	Set kV (kV)	Tube voltage (kV)	Exposure time (ms)	Exposure (mGy)	Exposure rate (mGy/s)	HVL (mm Al)
kVp accuracy						
	28	29,3261967	425,061401	3,684812741	8,617388864	0,352921546
	28	29,3048401	425,079987	3,690275415	8,629788023	0,352855414
	28	29,224205	424,564514	3,693587949	8,627879003	0,352720857
	28	29,3042831	425,05661	3,690426531	8,640755139	0,353016615
	28	29,3298721	425,061401	3,688191072	8,625289066	0,353034049
Half value layer	**Set kV (kV)**	**Tube voltage (kV)**	**Exposure time (ms)**	**Exposure (mGy)**	**Exposure rate (mGy/s)**	**HVL (mm Al)**
	22	23,0587215	316,163696	0,988715905	3,107053928	0,279150605
	25	26,3027802	368,853699	2,031711374	5,462765728	0,323161304
	28	29,224205	424,564514	3,693587949	8,627879003	0,352720857
	31	32,4441109	582,65387	6,992840646	11,95955848	0,377457231
	33	34,5612488	783,910706	10,56249807	13,4224152	0,392090231
Output	**Set kV (kV)**	**Tube voltage (kV)**	**Exposure time (ms)**	**Exposure (mGy)**	**Exposure rate (mGy/s)**	**HVL (mm Al)**
40mAs	28	29,3261967	425,061401	3,684812741	8,617388864	0,352921546
	28	29,3048401	425,079987	3,690275415	8,629788023	0,352855414
80mAs	28	29,2958794	845,11731	7,399984722	8,734942388	0,352961302
	28	29,3255577	845,633972	7,398645266	8,718107794	0,353176951
125mAs	28	29,2866421	1319,39197	11,57415499	8,759022456	0,353084981
	28	29,301815	1318,37	11,57439891	8,755846884	0,353030831

Appendix E4: Raw Data from CAR (continued)

AEC	Thickness (mm)	Set kV (kV)	Tube voltage (kV)	Exposure time (ms)	Exposure (mGy)	Exposure rate (mGy/s)	HVL (mm Al)
	30		25,77	1345	1,636	1,214	0,334
			24,92	1339	1,673	1,247	0,334
			25,76	1341	1,641	1,221	0,334
			25,73	1340	1,64	1,222	0,334
			25,78	1343	1,643	1,22	0,334
	45		25,74	1349	1,647	1,219	0,334
			25,23	1333	1,647	1,232	0,336
			25,02	1340	1,667	1,241	0,335
			25,92	1337	1,638	1,222	0,335
			25,98	1338	1,638	1,221	0,335
	70		25,89	1345	1,648	1,223	0,335
			25,06	1345	1,679	1,246	0,335
			25,51	1409	2,354	1,669	0,338
			26,15	1409	2,33	1,65	0,338
			25,58	1412	2,354	1,664	0,338

Appendix E5: Raw Data from CAR (continued)

MGD

	Thickness	Set kV (kV)	Tube voltage (kV)	Exposure time (ms)	Exposure (mGy)	Exposure rate (mGy/s)	HVL (mm Al)
Manual	30		25,1026173	517,4262085	2,891409738	5,566130317	0,316118509
	40		27,9234276	530,4786987	4,63651505	8,707325117	0,345665157
	45		28,9204998	578,1505737	5,763261479	9,92482481	0,35406962
	50		28,936779	578,1033936	5,767994512	9,933780377	0,354283929
	60		30,0378284	712,1400146	8,061494017	11,27984919	0,362741053
	70		30,0053101	902,8270874	10,22508974	11,28789092	0,362746507
	Thickness	**Set kV (kV)**	**Tube voltage (kV)**	**Exposure time (ms)**	**Exposure (mGy)**	**Exposure rate (mGy/s)**	**HVL (mm Al)**
AEC	30		26,0374947	1528,140991	3,229408364	2,109816922	0,326999694
	40		26,0331535	1528,135986	3,234535639	2,112415775	0,32689482
	45		26,0858974	1526,662964	3,2298232	2,110722258	0,326968938
	50		26,043602	1526,137939	3,242686052	2,121911424	0,327149689
	60		26,0889473	1526,128052	3,226137822	2,109696842	0,327321202
	70		26,105011	1525,13501	3,23282307	2,116848146	0,327371061

Appendix E6: Raw Data from CHUD/OP

	Set kV (kV)	Tube voltage (kV)	Exposure time (ms)	Exposure (mGy)	Exposure rate (mGy/s)	HVL (mm Al)
kVp accuracy	28	29,799	535,98999	3,946	7,31397434	0,35179821
	28	29,905	533,9729	3,928	7,32174861	0,35224268
	28	29,846	534,9953	3,936	7,32218213	0,35195979
	28	29,850	536,496216	3,953	7,32592494	0,3521187
	28	29,846	534,9953	3,936	7,32218213	0,35195979
	Set kV (kV)	**Tube voltage (kV)**	**Exposure time (ms)**	**Exposure (mGy)**	**Exposure rate (mGy/s)**	**HVL (mm Al)**
Half Value Layer	23	24,7215881	15,5820503	1,81617971	0,92792337	0,29721698
	25	26,9363918	1758,50598	1,46437288	0,83129879	0,32392535
	28	29,9610825	1628,48999	1,17369442	0,71960313	0,35269719
	31	32,8061333	1575,34399	1,00216671	0,63514619	0,37527287
	32	33,8228989	1563,78601	0,95617396	0,60968388	0,38233909
	Set kV (kV)	**Tube voltage (kV)**	**Exposure time (ms)**	**Exposure (mGy)**	**Exposure rate (mGy/s)**	**HVL (mm Al)**
Output						
40mAs	28	29,905	533,9729	3,928	7,32174861	0,35224268
	28	29,846	534,9953	3,936	7,32218213	0,35195979
80mAs	28	29,841	1072,97302	7,729	7,18307607	0,35205731
	28	29,841	1072,47595	7,731	7,18477724	0,3519474
130mAs	28	29,866	1724,85803	12,435	7,19469958	0,35221249
	28	29,856	1725,34595	12,437	7,1958636	0,35208285

Appendix E7: Raw Data from CHUD/OP (continued)

AEC

Thickness (cm)	Tube voltage (kV)	Exposure time (ms)	Exposure (mGy)	Exposure rate (mGy/s)	HVL (mm Al)
30	27,3090057	1727,90198	1,38356776	0,79932925	0,32835037
	27,8783283	1706,29395	1,34527034	0,78701339	0,33412695
	27,3278389	1719,849	1,33360426	0,77383518	0,32800058
	27,2830715	1718,33801	1,32601899	0,77032284	0,32779023
	27,4294243	1715,82495	1,3060701	0,75961155	0,32788795
45	27,3280182	1718,33301	1,32471123	0,76934088	0,32816121
	27,4431629	1715,33606	1,3019961	0,75790376	0,32810098
	27,2993526	1718,33301	1,32404284	0,76895271	0,32779893
	27,371788	1711,84802	1,28749918	0,75101072	0,32811928
	27,3644257	1726,38696	1,37182639	0,79322453	0,32851771
70	27,3647099	1717,36401	1,31619613	0,76528763	0,32792717
	27,256958	1723,854	1,35901395	0,78696923	0,3279146
	27,4323502	1719,35205	1,32853382	0,77154801	0,32824796
	27,4083576	1716,85596	1,31296892	0,76318623	0,32827556
	27,3269863	1718,31995	1,3296256	0,77219055	0,328008

Appendix E8: Raw Data from CHUD/OP (continued)

MGD - MANUAL

Thickness	Set kV (kV)	Tube voltage (kV)	Exposure time (ms)	Exposure (mGy)	Exposure rate (mGy/s)	HVL (mm Al)
30	31	33,1695862	572,629578	5,48765004	9,52467833	0,37763998
40	31,5	33,8139267	718,130798	7,22047985	10,0189062	0,3822135
45	32	34,2643471	903,332825	9,2164327	10,1682945	0,38503745
50	32	34,2660942	717,642212	7,3672258	10,2150884	0,3850753
60	32	34,1877823	717,660828	7,38231555	10,2432077	0,38478783
70	33	35,4391174	904,350586	10,0780929	11,1007969	0,39304349

MGD - AEC

Thickness	kVp_{dis} (kV)	kVp_{mea}(kV)	Exposure time (ms)	Exposure (mGy)	Exposure rate (mGy/s)	HVL (mm Al)
30	25,5	27,3090057	1727,90198	1,38356776	0,79932925	0,32835037
40	25,5	27,4210377	1722,37695	1,3508281	0,78267094	0,32823411
45	25,5	27,4431629	1715,33606	1,3019961	0,75790376	0,32810098
50	25,5	27,3802185	1718,81702	1,32371894	0,76853842	0,32824755
60	25,5	27,3602104	1715,33704	1,30598103	0,76022303	0,32818583
70	25,5	27,4323502	1719,35205	1,32853382	0,77154801	0,32824796